Review of QCD at LEP

W. de Boer
Univ. of Karlsruhe *

1 Introduction

We review the first round of QCD studies at the e^+e^- collider LEP, which started operating towards the end of last year. These studies at the peak of the Z^0 resonance have proven to be extremely rewarding, not only because of the large statistics available due to the high resonance cross section, but also because of the higher centre of mass energy, which allows a much cleaner study of events with multiple jets. For example, 20% of the events show a clean 3-jet structure in which the least energetic jet has an average energy of 20 GeV. Such events originate from quark-antiquark-gluon ($q\bar{q}g$) states, in which the least energetic jet is usually the gluon jet. Therefore, at LEP energies the gluon jets are considerably 'healthier' than at the PEP and PETRA colliders, where the energies were typically three times lower. The higher jet energy gives a better collimation of the jets and therefore a better jet axis determination and separation between the jets. This improves many QCD studies, especially the study of gluon jets and the angular correlations in 4-jet events, from which one can hope to isolate the triple gluon vertex contribution. This gluon self interaction is the hallmark of the non-abelian character of QCD and is thought to be responsible for the confinement of quarks inside the nuclei.

The topics to be discussed here are:

- Intermittency
- Charged multiplicity and rapidity distributions
- Comparison with fragmentation models
- Soft gluon coherence
- Jetmultiplicity studies and the determination of α_s
- Determination of α_s from the asymmetry in energy-energy correlations
- Search for the triple gluon vertex

*Invited talk at the Topical Conference of
the eighteenth SLAC Summer Institute on Particle Physics, Stanford, August 1990
Bitnet: DEBOERW@CERNVM
Postal address: Inst. für Experimentelle Kernphysik
Univ. Karlsruhe, Postfach 6980, D-7500 Karlsruhe

2 Intermittency

Intermittency studies search for charged multiplicity spikes or more formal, correlated density fluctuations, in phase space bins, e.g., rapidity bins (δy) or 2-dimensionally rapidity and azimuth bins. Instead of studying the average multiplicity per bin, one usually studies the factorial moments of rank q, denoted by F_q, which are proportional to $n \cdot (n-1) \cdots (n-q+1)$. They measure the probability to have more than $q-1$ particles in the bin, e.g., F_3=0 if there are no bins with more than 2 particles. Of course, this depends on the bin size, so one studies F_q as function of bin size. The advantage of the factorial moments, introduced by Bialas and Peschanski[1], are that they are very sensitive to possible new effects and that in simple models clear predictions exist for the slopes of F_q as function of bin size. For example, for uncorrelated hadron production the slopes are zero, while for self-similar cascading models they follow a power law behaviour. Large intermittency effects are usually meant to be equivalent with large slopes, especially for small bins.

The interest in intermittency studies has been the observation of large intermittency effects in $p\bar{p}$ collisions, cosmic ray events, nucleus-nucleus collisions, hadron-hadron collisions, and e^+e^- annihilation, which could not be explained by Monte Carlo predictions. This has led to speculations about possible evidence for hadronic phase transitions[2], hadronic Cherenkov radiation[3], hadronic hydrodynamics[4] (the name intermittency originates from turbulence theory in fluid dynamics), or fractal structures in hadronization[1,5]. For details we refer to recent reviews[6] and references therein.

Here we will concentrate on the study of intermittency in e^+e^- annihilation, in which the intermittency effects are found to be largest. The DELPHI Collaboration[7] has searched for intermittency effects in Z^0 decays. They found that the observed power law behaviour of F_q could be well described by the current hadronization models (see Fig. 1) in contrast to earlier results by the TASSO Collaboration[8] at a centre of mass energy of 35 GeV, who only observed qualitative agreement with their Monte Carlo models.

Recently there has been a nice analysis by the CELLO Collaboration[9] about intermittency in three dimensions and they find at 35 GeV a strong intermittency signal, which is in agreement with Monte Carlo too, so both at 91 and 35 GeV there seems to be no contribution to the intermittency outside the well known correlations from resonances, decays, and energy-momentum conservation. The intermittency in three dimensions is stronger, since the saturation effects through projection on a single axis are less severe in two or three dimensions. Also the HRS Collaboration has analysed their data at $\sqrt{s}$ = 29 GeV and observe a strong intermittency signal, but they do not make a comparison with Monte Carlo models[10].

Bose-Einstein correlations appear to play a minor role in the intermittency, as shown already in the Physics at LEP study[11]. In this study it was shown too, that Monte Carlo models based on the exact second order QCD matrix element and the ones based on the Leading Log parton showers gave completely different predictions for the factorial moments at LEP energies. It was shown by DELPHI[7], that the large difference disappears or even becomes of opposite

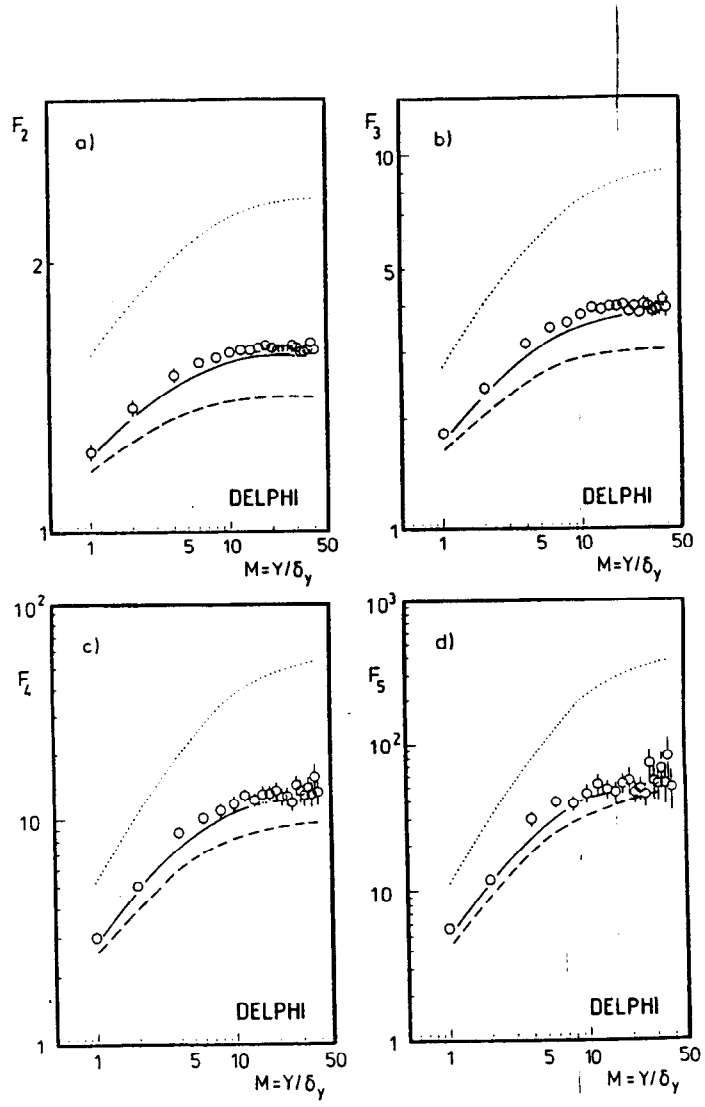

Figure 1: Dependence of factorial moments of rank 2 (a), 3(b) 4 (c) and 5 (d) on the number M of subdivisions in the rapidity interval for data at 91 GeV (DELPHI). The curves are the expectation from the Lund Parton Shower model (solid line), and the matrix element Monte Carlo before (dotted line) and after retuning (dashed line) of the rapidity distribution.

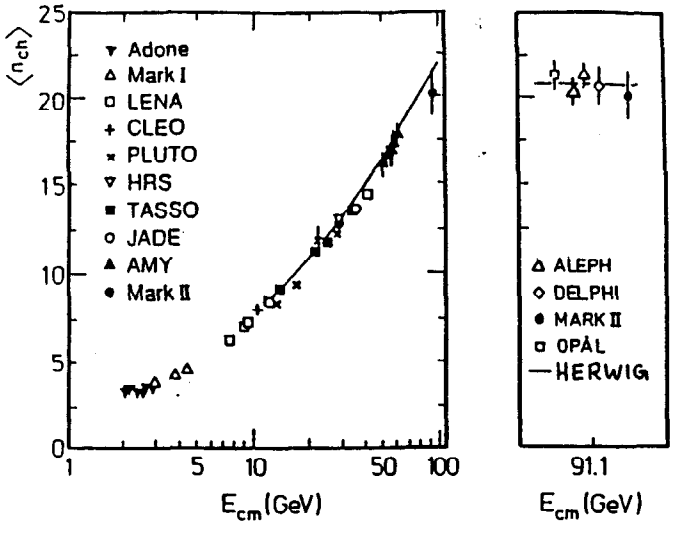

Figure 2: The averaged charged particle multiplicity in e^+e^- annihilation as function of the centre of mass energy with the prediction of the Lund Parton Shower model (a) and the same at 91 GeV with the prediction of the HERWIG Monte Carlo (b).

sign by a slight retuning of the fragmentation parameters in order to describe the rapidity and aplanarity distributions at 91 GeV (see Fig. 1). The main effect of this retuning is to lower the particle density in a jet somewhat by increasing the transverse momenta from 350 to 500 MeV and decreasing the averaged momentum in order to increase the charged multiplicity from 18 to the observed multiplicity of 21. Such minor changes reduce F_2 by more than 50% and change the slopes too! This indicates the sensitivity of the factorial moments to the tuning of Monte Carlo parameters. Before one claims new physics not described by Monte Carlo, one should make sure one cannot make the discrepancy between data and Monte Carlo go away by a slight retuning of the Monte Carlo parameters. Since the intermittency is well described by Monte Carlo, the CELLO Collaboration has searched for the effect in the Monte Carlo and find that the rising slopes in F_2, even for small bin sizes, can be mainly attributed to the Dalitz decays $\pi_0 \to e^+e^-\gamma$. If these decays are switched off in the Monte Carlo, F_2 becomes constant for small bin sizes.

3 Charged Particle Multiplicities

At any new accelerator the measurement of the charged multiplicity distribution has always been of interest in order to compare it with lower energies and with other reactions. It is of special interest to see if the negative binomials, expected

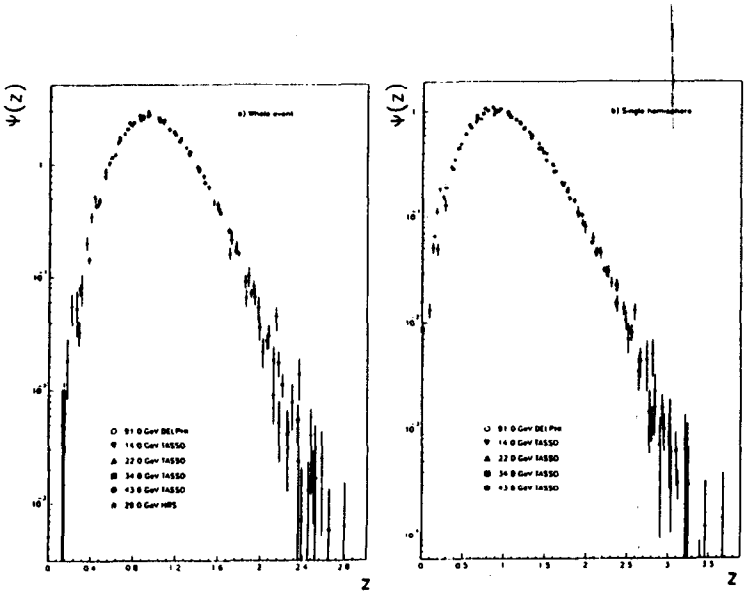

Figure 3: The KNO distribution of charged particle multiplicities divided by the averaged multiplicity $z = N_{ch}/N_{av}$ in e^+e^- annihilation for various centre of mass energies.

in QCD[12], can still describe the data or to see if KNO scaling[13] still holds. If KNO scaling holds, the multiplicity distribution normalized to the averaged multiplicity should be independent of energy. Fig. 2 shows the charged multiplicity as function of centre of mass energy compared with the Monte Carlo prediction of the parton shower model from the LUND group[20] (taken from Ref. [14]). Table 1 summarizes the averaged multiplicities of the various experiments[15]-[19]. The average of 20.7±0.4 is in good agreement with the expectations of 21.2 from the JETSET[20] - and 20.8 from the HERWIG[21] Monte Carlo. The DELPHI Collaboration has studied the multiplicity and rapidity distributions in detail[18]. They find:

- KNO scaling holds reasonably well (see Fig. 3). It is interesting to note that the KNO scaling function is close to the lognormal distribution, expected

MARK – II	$20.1 \pm 1.0 \pm 0.9$	*ALEPH*	$20.36 \pm 0.06 \pm 0.79$
DELPHI	$20.71 \pm 0.04 \pm 0.77$	*OPAL*	$21.28 \pm 0.04 \pm 0.84$
$< N_{ch} >$	20.7 ± 0.4		
JETSET PS	21.2	*HERWIG*	20.8

Table 1: Charged particle multiplicities at the Z^0 resonance.

in self similar models[22].

- The negative binomial distribution needs a modification in order to give a good description (see Fig. 4).
- The predictions of the model of Ellis et al.[23] give the right averaged multiplicity, but the distribution is somewhat wider (see Fig. 4).
- the slopes of the coefficient in the negative binomial distribution (1/k) are different for μp and e^+e^- (see Fig. 5).

4 Comparison with Monte Carlos

The Monte Carlo simulation of hadronic final states in e^+e^- annihilation consists of four phases:

1: Primary quark production.
The annihilation of the e^+e^- into a photon or Z^0, followed by the production of a $q\bar{q}$ pair of a given flavour. These diagrams are well understood and the Standard Model gives precise predictions.

2: Perturbative radiation of photons and gluons.
After the production of $q\bar{q}$ pairs, the accelerated quarks can radiate photons and gluons. The final state photon radiation by quarks can be very well studied on top of the Z^0-resonance, since initial state radiation is small in this case and first results have been obtained by OPAL[24]. The results are in agreement with perturbative calculations. Gluon radiation can also be calculated perturbatively[25], as long as the strong coupling constant is still rather small, i.e., for hard gluons with a large Q^2. For small Q^2 the coupling increases towards infinity, which causes the confinement of quarks inside hadrons. The perturbative radiation of gluons is either calculated according to the exact second order QCD matrix element (ME) or using the Leading Log Approximation (LLA). The LLA allows the calculation of any number of collinear or soft gluons (developing into a parton shower), but the approximation is not valid for hard gluons. Therefore, hard gluons have to be treated specially. For example, in the parton shower model of the LUND group (version JETSET 7.2) the radiation of the first gluon is treated according to the first order QCD matrix element[20]. In the HERWIG Monte Carlo the parton shower is only based on the LLA, followed by cluster fragmentation[21]. The JETSET 7.2 program from the LUND group has the exact second order matrix elements available as options (both the GKS-[26] and the more accurate ERT matrix element[27] are available).

3: Hadronization.
In this non perturbative regime one has to resort to phenomenological models, like string -, or cluster fragmentation. A rather complete overview has been given in the Yellow Book on Physics at LEP[11], while the underlying physics concepts have been well explained in a review by T. Sjöstrand[28].

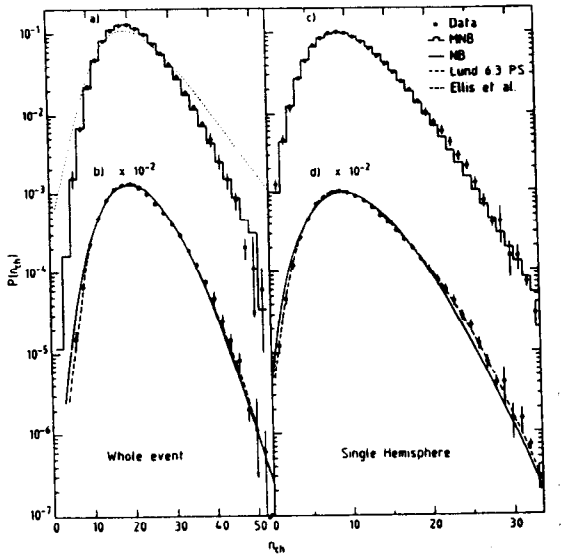

Figure 4: The charged particle multiplicity distribution compared with the negative binomial distributions in e^+e^- annihilation at 91 GeV.

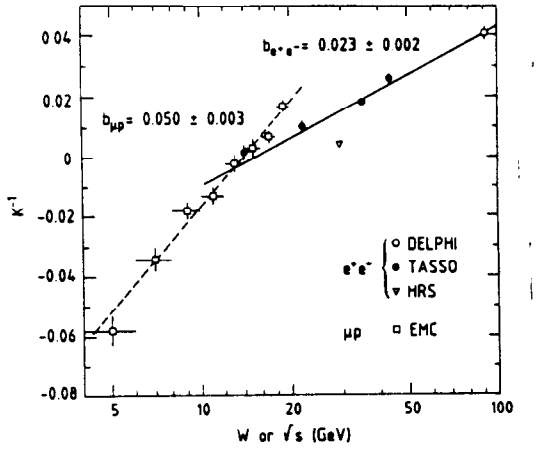

Figure 5: The slopes of the coefficients in the negative binomial distribution for μp scattering and e^+e^- annihilation.

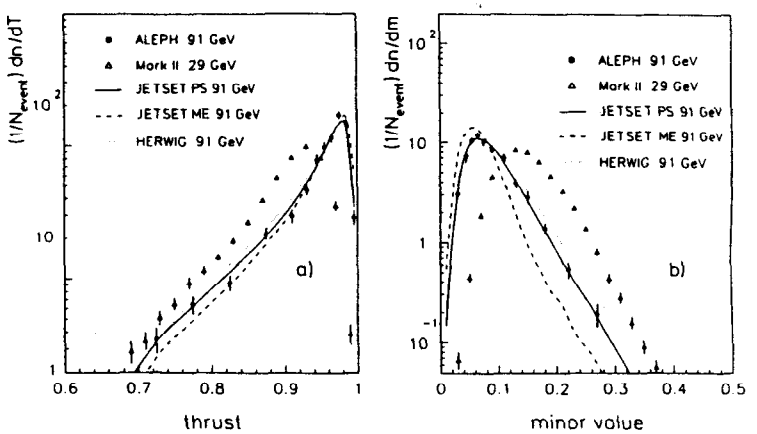

Figure 6: Comparison of the thrust and minor value at 29 and 91 GeV. Data from MARK-II and ALEPH.

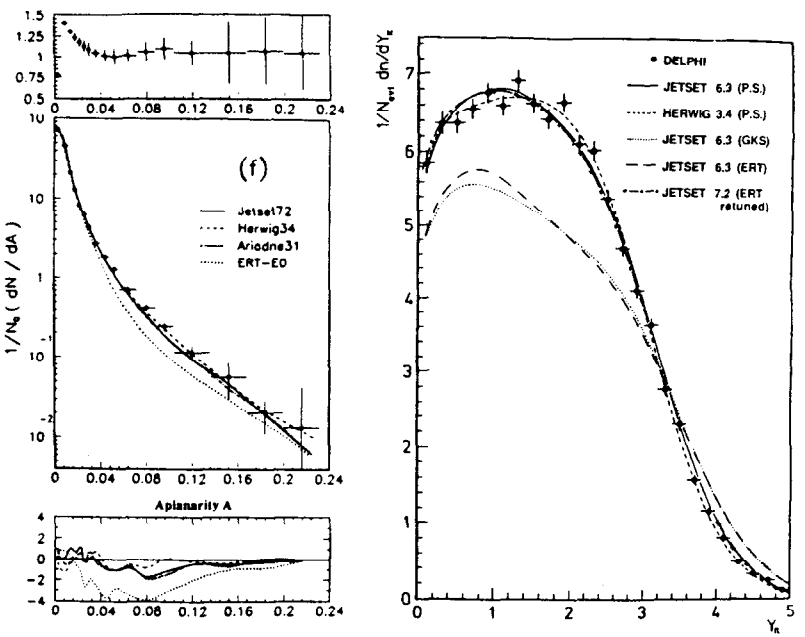

Figure 7: Comparison of the aplanarity- (OPAL) and rapidity (DELPHI) distribution at 91 GeV with various Monte Carlo models. The 'ERT retuned' curve for the rapidity uses retuned parameters for the matrix element at 91 GeV and is close to the curves for the parton shower models.

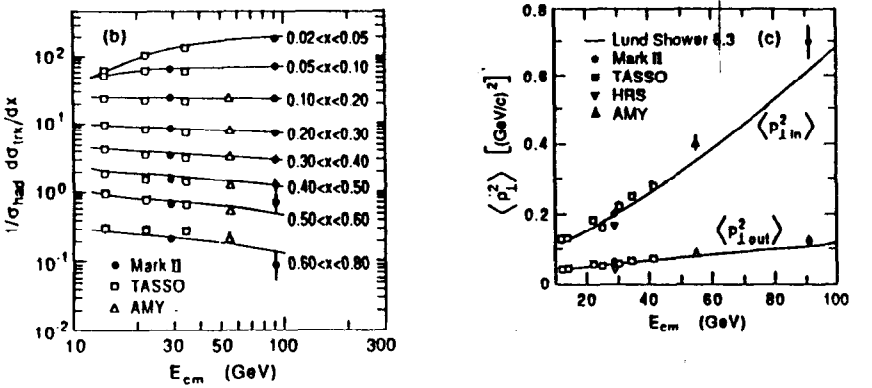

Figure 8: The particle density for various $x = p/E_{beam}$ bins as function of centre of mass energy.

4: Decays of unstable hadrons and specific detector simulation.

The parton shower models with the fragmentation parameters determined at PEP and PETRA energies appeared to describe reasonably well the data at the Z^0-resonance[15,16,17,18,19], as shown in Figs. 6 and 7. Note that the thrust and minor values are narrower at the higher energies, indicating that the jets become narrower and more planar. The models based on the exact second order matrix element could not describe the data at the higher energies with the parameters from the lower energy data. Especially the aplanarity and rapidity could not be described, as shown in Fig. 7. The curves labeled 'ERT' or 'GKS' correspond to the matrix element models, the other curves are from the parton shower models. After a retuning of the fragmentation parameters, the agreement became much better (see Fig. 7b). The need for the retuning in the matrix element model could be traced back to the fact that the Q^2 evolution of the fragmentation process, as predicted by the Altarelli-Parisi equations[29], has been implemented in the parton shower models, but not in the ME programs. This is a large effect, if one goes from PETRA to LEP energies, as shown by the first data from MARK-II[15] (see Fig. 8): the number of particles with small $x = p/E_{beam}$ increases more than 50%, while the high momentum particles decrease by about 50%. The physical picture is clear: more (mainly soft) gluons are emitted at higher energies, where more phase space is available. The soft gluons fragment into soft hadrons, while simultaneously the fractional energy left over for the primary quarks becomes less, thus requiring a softer fragmentation function.

By retuning the fragmentation functions in the ME models in order to take into account the Q^2 evolution, the agreement between the PS and ME models became much better[30], provided the definition of the strong coupling constant is similar in both cases, i.e., α_s should be evaluated at a scale of a few GeV, which is typically the Q^2 of the gluon emission. In the newest version JETSET 7.2 of the ME Monte Carlo from the LUND group it has become possible to choose the

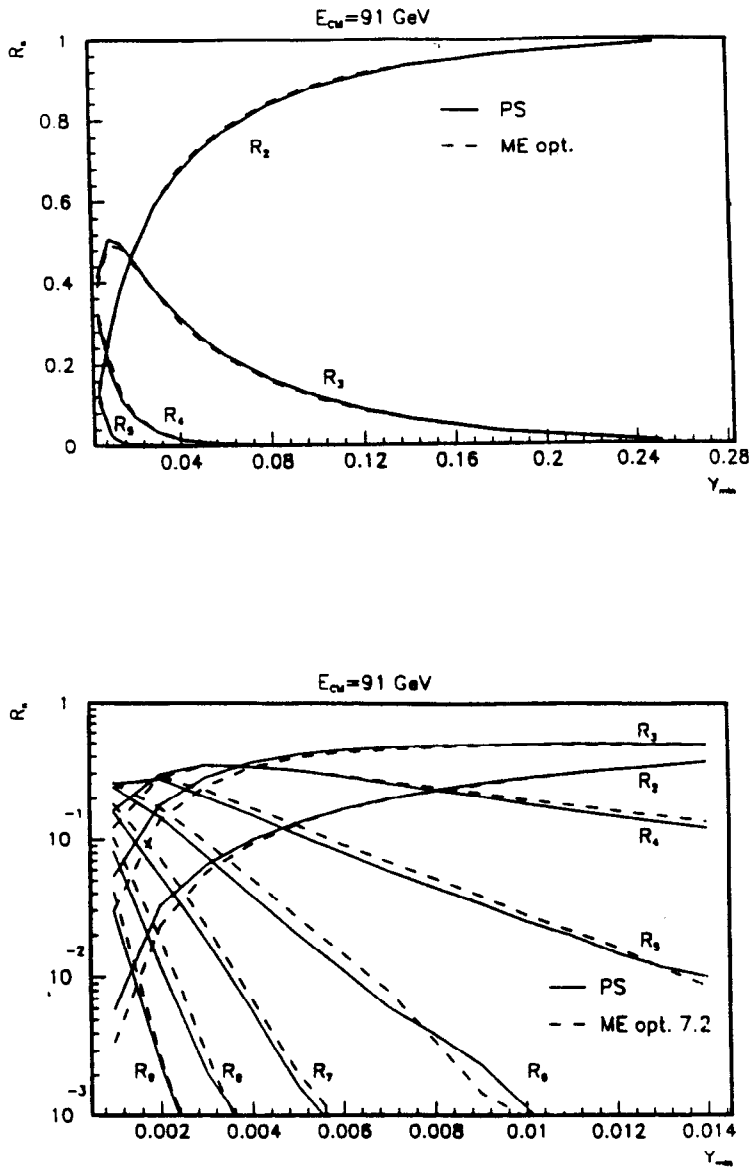

Figure 9: **The jetmultiplicities at 91 GeV as function of the jet resolution $y_{min} = M_{ij}^2/s$ for the parton shower model and the exact matrix element with retuned parameters (both JETSET 7.2).**

	a	b	Λ_{LL1}	σ_q
DEFAULT(MKII PR D37(1988)1)	0.5	0.9	0.400	0.35
TASSO (ZP C41(1988)375)	0.18	0.34	0.260	0.39
OPAL (CERN – EP/90 – 48)	0.18	0.34	0.290	0.37

Table 2: **Longitudinal- (a and b) and transverse (σ_q) fragmentation parameters and QCD scale (Λ_{LL1}) used in the Lund parton shower model.**

scale as a fraction of the centre of mass energy; before α_s was always evaluated at $Q^2 = s$. A small scale is needed to describe the higher jet multiplicities[31], as will be discussed in more detail in Sect. 7. Note that the necessity for a small scale is not a feature of the ME Monte Carlos, also in the PS models one has to choose the scale to be of the order of the p_t^2 of the gluon in order to describe the data.

Although the global features of the LEP data were quite well described by the default parameters of the Lund parton shower model JETSET 7.2, it needed still some retuning, especially the 3-jet rate came out too high, indicating a too large value of the QCD scale. The OPAL Collaboration[19] has published their optimized values of the parameters and they find the QCD scale to be 290 MeV instead of the default value of 400 MeV. This value is close to the value published by the TASSO Collaboration[32] from data at 35 GeV, but differs from the one by the MARK-II Collaboration[33] obtained at 29 GeV. The latter one has been taken as default in JETSET 7.2. The differences have been summarized in Table 2. Note that the value of the QCD scale in the PS model is not $\Lambda_{\overline{MS}}^{(5)}$, but something I have denoted with Λ_{LL1}, since this program is based on a combination of the Leading Log Approximation and the first order QCD matrix element. For example, a value of Λ_{LL1}=260 MeV corresponds to $\Lambda_{\overline{MS}}^{(5)}$=100 MeV in the ME Monte Carlo[30]. After retuning its parameters, the ME model agrees reasonably well with the PS option, at least in the regions where hard gluons dominate[30]. Especially the jet rates are in good agreement, even up to 9-jet final states, as shown in Fig. 9.

The jet multiplicities of 5 or higher start to be present only for y_{cut} below 0.01, i.e., in the fragmentation region, where the jet masses start to be important. In the ME option at most 4 jets are generated at the parton level, but fragmentation generates the higher jet multiplicities just as well as the PS option. Note that the fraction of 4-jets is small, as expected from the fact that α_s^3 is a small number. This is the main reason why the ME models can describe the event shapes in the regions where hard gluons dominate.

5 Coherence of Soft Gluons

The OPAL collaboration[34] has made a comparison of the hadron momentum spectra with the predictions based on leading log calculations including the interference between soft gluons, as calculated by the Leningrad groups[35]. They find that the expected peak in the ln p spectrum is well reproduced by the data over

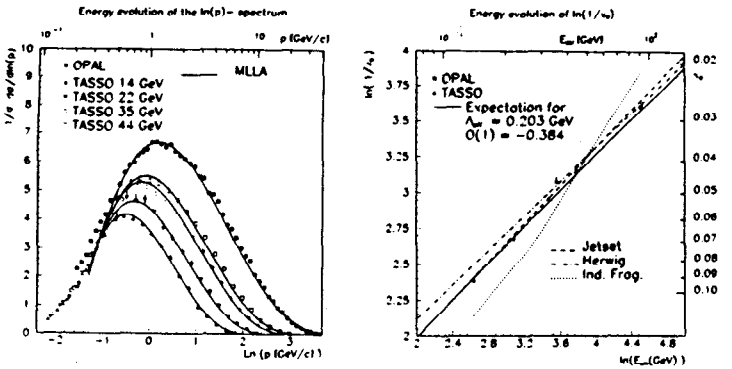

Figure 10: The charged particle momentum spectra for various centre of mass energies (a) and the behaviour of the peak as function of centre of mass energy (b).

the whole energy range between 14 and 91 GeV, as shown in Fig. 10. Note that these predictions have only one single parameter - apart from the overal normalization - and therefore the comparison is non-trivial. Without interference the spectra would not decrease so strongly for low momenta.

However, the suppression of the low momentum particles is in the region where the hadron masses play a role and the theoretical formulae are only valid in the region where the momenta are much larger than the hadron masses. Decays of massive particles cause a decrease of the low momentum particles and indeed Monte Carlos without interferences show a large suppression of these low momentum particles too. Therefore, a more sensitive test is the study of the peak shift as function of $\sqrt{s}$.

The energy dependence of the peak of the ln p spectrum can only be described by Monte Carlo models including the interference effects, either by the angular ordering of the gluon emission in parton showers or by the string effect or by both (see Fig. 10b). As an alternative model without interference one could try to use independent fragmentation models. However, they exist only in matrix element versions without Q^2 evolution, so they do not describe the energy dependence. Therefore, OPAL has tried to replace the string fragmentation in the parton shower models by independent fragmentation, since in this case the Q^2 evolution is taken into account. They find that such a model without interferences does not reproduce the energy dependence (see Fig. 10b), but is much closer to the slope of 1 expected if the spectrum of soft particles is dominated by phase space effects.

Although it is difficult to call the behaviour of the momentum spectra as function of energy evidence for the colour coherence in QCD, because of the finite energies where mass effects are still important, this is again a case where QCD cannot be proven, but it does a wonderful job in describing the data.

6 String Effect and Gluon Fragmentation

One of the interesting aspects of QCD studies at 91 GeV is the fact that the gluon jets are 'healthier' than at PEP- and PETRA energies, as mentioned in the introduction. For example, typical gluon jet energies are 20 GeV for reasonably efficient jet selections (20% 3-jet events!), as shown in Fig. 11. Here the jet energy has been determined from the angles between the jets:

$$E_j = \frac{\sin\theta_{k,l}}{\sin\theta_{1,2} + \sin\theta_{2,3} + \sin\theta_{3,1}} E_{cm} \qquad (1)$$

with $(j,k,l) = (1,2,3)$ and permutations. At PEP - and PETRA energies the maximum possible gluon energy was around 10 GeV (in the so-called MERCEDES events n which all three partons have the same energy); the higher jet energies at LEP yield a better collimation of jets and therefore a better separation between the jets. These facts make it interesting to repeat the well known studies at lower energies concerning the particle flow in 3-jet events[36] and the difference between quark and gluon jets[37], especially since the results on the last topic have not been very conclusive.

6.1 String effect

The DELPHI Collaboration has started these studies[38] at LEP. To define jets they have used the LUCLUS algorithm, which is part of the LUND Monte Carlo[20]. This cluster algorithm starts to cluster around the most energetic particles and joins other particles according to a measure closely related to the p_t of the particles [1] in contrast to the popular 'JADE' cluster algorithm, which starts the clustering of particles with the lowest invariant masses and therefore starts usually with the soft particles first and clusters the more energetic particles around these soft particles. Furthermore, in this algorithm the particles cannot be reassigned to another cluster, which causes particles in opposite directions of the jet axis to stay within that jet, thus generating artificially broad jets [39].

The particle flow in 3-jet events exhibits the so-called string effect: in the event plane determined by the two vectors corresponding to the two largest values of the sphericity tensor, the particle flow around the most energetic jet shows an asymmetry. This effect, first observed by the JADE collaboration at PETRA energies and later on confirmed by others[36], is shown for the DELPHI data in Fig. 12. together with Monte Carlo curves from string fragmentation (SF) and independent fragmentation (IF) models. In this figure the most energetic jet is aligned at 0° and the angles of the particles in the event plane are measured with respect to this jet axis with the positive direction given by the second most energetic jet, which peaks at 120°. The valley between the two most energetic jets at 80° has clearly less particles than the valley at 270°. The string fragmentation model describes this asymmetry well in contrast to independent fragmentation, hence the name "string" effect.

There are several contributions to the "string" effect:

[1] They used the default option in LUCLUS with the DJOIN parameter set to 5 GeV, which yields a 3-jet rate of about 20% of the total number of events.

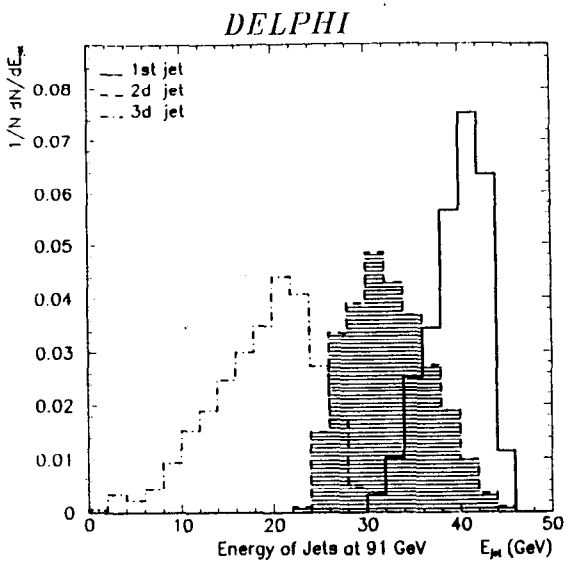

Figure 11: The energies of the three jets in 3-jet events selected with the Lund jet finder LUCLUS with $d_{join} = 5$ GeV. Data from DELPHI.

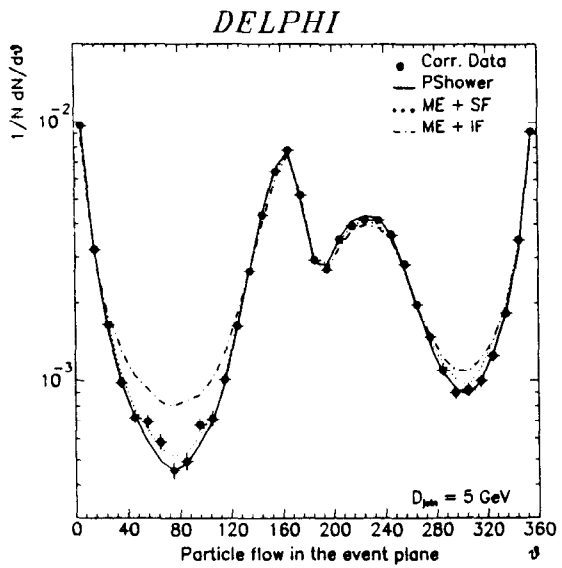

Figure 12: The particle flow in 3-jet events. Data from DELPHI.

1) The "drag" effect , i.e., particles are dragged towards the side of the gluon radiation by the boost of the string.

2) Interference effects at the parton level. This has been forwarded as a "QCD" explanation why the string picture works so well[40]-[43].

3) The "showering effect", i.e., a hard gluon radiated on one side can be split into several other partons, thus spilling particles on one side of the hardest jet, but hardly on the other side.

In the ME option the whole string effect has to be attributed to the 'drag' effect, since at the parton level this effect is practically absent.

A Monte Carlo study reveals that in the parton shower model most of the string effect is already present at the parton level, at least if a small cutoff for the stopping point of the shower is used. Therefore the 'drag' effect hardly contributes in this case; at the parton level both the showering effect and interferences can contribute.

The interference effects, as implemented in the Monte Carlos by angular ordering of the gluon emission, turn out to have little influence on the string effect[2] [42,38]. Naively, one would conclude that the showering effect would then dominate. However, according to the experts[41] the angular ordering is only related to the interferences *within* a jet, while the string effect is only related to the interferences *between* the jets. These are called the intra-jet and inter-jet interferences, respectively. In how far the 'inter-jet' interferences have been implemented in the shower Monte Carlos is not clear. Therefore, it is not clear how much of the string effect at the parton level is due to the 'showering' effect and how much is due to the inter-jet interference.

It is interesting to note, that the so-called 'Modified Independent Fragmentation' models can describe the string effect too[44]. In these models the p_t^2 of the particles is made dependent on the longitudinal momentum in such a way, that it happens to reproduce the coherence effects[45]. However, it still remains to be seen, if these models can describe other aspects of the event shapes in e^+e^- annihilation too.

6.2 Gluon fragmentation

The least energetic jet in 3-jet events is most likely the one closest to the original gluon direction. A Monte Carlo study reveals that this happens in 53% of the cases, while the probability for the first and second jet to be the gluon is 18% and 25%, respectively. So one can compare the properties of the third jet with respect to the first two jets to search for differences between quark and gluon jets.

Fig. 13 shows the opening angles of particles inside the jets. All jets have the same distribution above 20°, but below 20° the third jet has a factor three less particles than the first two ones. Such a depletion is expected for gluon jets, since gluons most likely split into other gluons before fragmenting, thus naively yielding broader jets and a lower "core" density. To see if this depletion is really due to a

[2] Within the JETSET 7.2 program the angular ordering can be switched on and off[20].

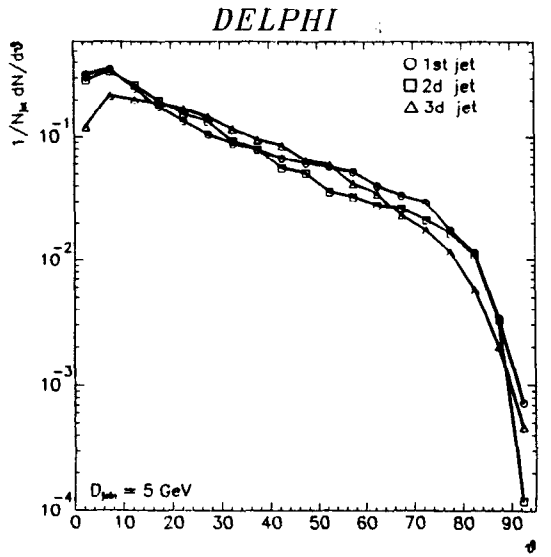

Figure 13: The distribution of opening angles of the particles in the three jets of 3-jet events. Data from DELPHI.

difference between gluon and quark fragmentation, one has made a Monte Carlo comparison between the gluon jet at $\sqrt{s} \simeq 91$ GeV with quark jets in 2-jet events at $\sqrt{s}$=40 GeV and quark jets in 3-jet events at $\sqrt{s}$=60 GeV. In all cases the jet energies are approximately 20 GeV (in the 3-jet case at 60 GeV the second jet was taken).

The 20 GeV *quark* jet in a 3-jet environment agrees reasonably well with a 20 GeV *gluon* jet, but a 20 GeV *quark* jet in a 2-jet event shows a considerably different angular distribution. The differences between the two quark jets of 20 GeV in Fig. 14 can be explained as follows: At large angles it is probably connected with the larger angular range available in 2-jet events, since in 3-jet events particles at angles above 70° are likely to be associated to other jets. In the range from 20°-50° the strings in the 3-jet events "drag" more particles into this region, thus causing a quark jet in a 3-jet event to look more like a gluon jet.

This study clearly shows that it is difficult to talk about "the" quark fragmentation: in general the fragmentation depends on the environment in which the quark is imbedded, as expected since isolated quarks do not exist if confinement holds. All one can say is that the current string fragmentation models describe the fragmentation of both quarks and gluons very well in all environments.

7 Jetmultiplicities

The motivation for studying jet multiplicities has been twofold:

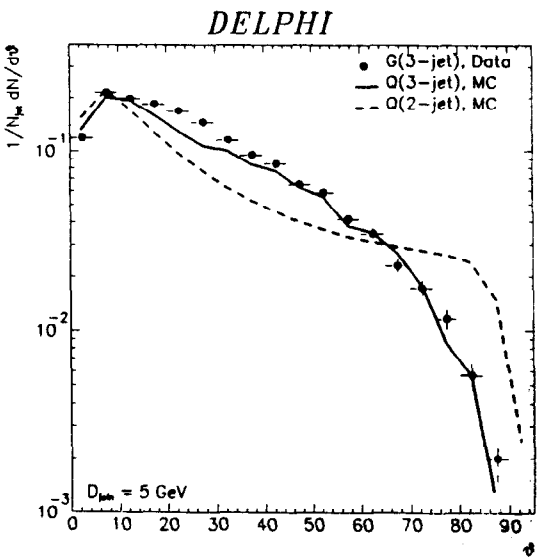

Figure 14: A comparison of the opening angles in a 'gluon' jet at 91 GeV, a 'quark' jet in 3-jet events at 61 GeV, and a 'quark' jet in 2-jet events at 40 GeV, as obtained from the ME JETSET 7.2 Monte Carlo. In all cases the jet energies are around 20 GeV.

- The relative jet rates are determined by α_s, thus providing the possibility to determine this fundamental constant.
- The running of α_s can be proven by studying the 3-jet rate (R_3) as function of centre of mass energy.

R_3 is shown as function of $\sqrt{s}$ in Fig. 15 for energies between 14 and 91 GeV using data from PEP, PETRA, KEK, and LEP, as compiled by S. Bethke[46]. Amazingly, all experiments have been able to use the same definition of R_3, i.e., the same jet finder, namely the one introduced by the JADE Collaboration[47]. The first data at 91 GeV, as obtained by OPAL[49], clearly established the decrease of R_3 in agreement with the running of α_s as expected in QCD. Lateron, the jet rates at 91 GeV were confirmed by the DELPHI[50] and L3[51] collaborations. In first order $\alpha_s(\mu) \propto 1/\ln(\mu)$. Therefore one expects a straight line, if the 3-jet rate is plotted as function of $1/\ln(E_{CM})$. Indeed, the data is well described by such a straight line, as shown in Fig. 15b (from [48]). The line is compatible with going through the origin, i.e., a vanishing α_s for infinite energies, as expected from the concept of asymptotic freedom.

The determination of α_s turned out to be more tricky. The $\Lambda^{(5)}_{\overline{MS}}$ values quoted by DELPHI[50], L3[51], MARK-II[52], and OPAL[49,53], can be summarized as:

$$80 < \Lambda^{(5)}_{\overline{MS}} < 350 \text{ MeV}.$$

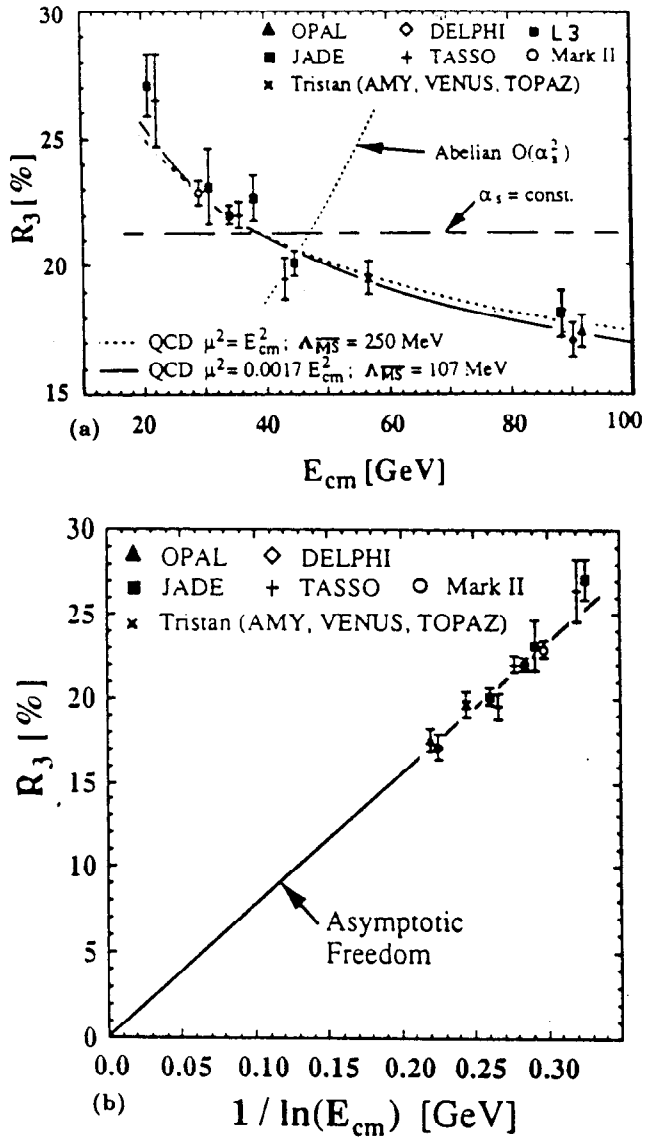

Figure 15: **The fraction of 3-jet events as function of centre of mass energy (E_{CM}) (a) and as function of $1/\ln(E_{CM})$ (b).**

The spread in $\Lambda^{(5)}_{\overline{MS}}$ originates from three sources:

- The fitting procedure.
- The renormalization scale dependence, i.e., choice of scale in the definition of α_s.
- The recombination scheme dependence, i.e., which cluster algorithm is used to define the jets.

All three points are interrelated, since e.g., different recombination schemes show a different dependence on the renormalization scale. Some people call this the recombination scheme dependence, others claim there is no recombination scheme dependence, only renormalization scale dependence. Let me discuss these problems first separately.

7.1 Renormalization scale dependence

The definition of the strong coupling constant involves two scales: one is an unphysical renormalization scale μ used to regularize the infinities in the loop corrections and then the physical Q^2 scale. One can trade the renormalization scale μ for a μ independent QCD scale Λ[54], in which case one finds up to order $O(\alpha_s^2)$:

$$\alpha_s(Q^2) = \frac{4\pi}{\beta_0 L}\left[1 - \frac{\beta_1}{\beta_0^2}\frac{lnL}{L}\right] \qquad (2)$$

with

$$\begin{aligned} L &= \ln(Q^2/\Lambda^2_{\overline{MS}}) \\ \beta_0 &= 11 - \tfrac{2}{3}n_f \\ \beta_1 &= 2(51 - \tfrac{19}{3}n_f) \end{aligned} \quad .$$

We will use the usual $\overline{MS}$ renormalization scheme[55]. Since α_s depends only on the ratio of Q^2 and $\Lambda^{(5)}_{\overline{MS}}$, a different choice of renormalization scheme or scale, i.e., of $\Lambda^{(5)}_{\overline{MS}}$, can be compensated by a different choice of Q^2. Therefore, studying the renormalization scale dependence can be done by defining $Q^2 = f \cdot s$, where f is a renormalization scale factor.

The number of flavours n_f=5 at $Q^2 = M_Z^2$, but for a choice of Q^2 below the b-mass one has n_f=4. The unphysical jump in α_s, if one crosses a new quark threshold, can be compensated by a corresponding change in $\Lambda^{(5)}_{\overline{MS}}$[54], hence the upper index in $\Lambda^{(5)}_{\overline{MS}}$ indicates the number of flavours used. Although in the Monte Carlo's the scale factor f is typically so small, that n_f=4 should be used, we will follow the usual practice and quote the final results for $Q^2 = M_Z^2$ and n_f=5. The simple relation between $\Lambda^{(5)}_{\overline{MS}}$ and $\Lambda^{(4)}_{\overline{MS}}$ is given in Ref. [54].

Physical observables are independent of f, if they are calculated to all orders. In finite order perturbation theory there exists some dependence on f and several choices of f have been proposed[56,57,58] in order to minimize the sensitivity to higher orders. Instead of choosing such a particular scale, one better studies the scale dependence for a reasonably large range, which can be easily done as follows. Suppose an observable has been calculated up to second order:

$$O = C_1\alpha_s + C_2\alpha_s^2. \qquad (3)$$

If one chooses a different scale $Q'^2 = f \cdot Q^2$, one obtains from the renormalization group equation (or from its solution, Eq. 2) a change $d\alpha_s$ in the coupling constant:

$$d\alpha_s = -\beta_0 \alpha_s^2 \ln f + O(\alpha_s^3) \quad . \tag{4}$$

To keep the observable the same, one has to absorb the change in α_s in different coefficients C_1' and C_2', i.e.,

$$dO = \alpha_s \cdot dC_1 + C_1 \cdot d\alpha_s + \alpha_s^2 \cdot dC_2 + O(\alpha_s^3) = 0. \tag{5}$$

Since each power of α_s has to be zero, this yields: $C_1' = C_1$ and $C_2' = C_2 + \beta_0 \cdot C_1 \cdot \ln f$. As expected, the first order coefficient is independent of the scale, since the loop corrections only enter in second order.

For a given observable and scale one can solve Eq. 3 for α_s and calculate the corresponding $\Lambda_{\overline{MS}}^{(5)}$; the result is shown in Fig. 16 for $x = \sqrt{f}$ between 0.04 and 1 for the jetmultiplicities and the asymmetry in the energy-energy correlations, both to be discussed below. One observes a stronger scale dependence for the jet rates due to the larger second order corrections, which have been indicated in the figure too and were obtained from Refs. [59,60].

This dependence is calculated at the parton level. A different choice of scale leads to different higher order corrections, as can be easily seen from the expression for C_2' given above. At the hadron level part of the higher order corrections are absorbed in the fragmentation part and the renormalization scale dependence at the hadron level can be considerably smaller, if one requires that for different choices of scale the fragmentation parameters are retuned to get the right momentum spectra. This can be easily done, if one fits with the full Monte Carlo, as will be discussed below.

7.2 Fitting Procedures

In order to compare QCD with data, one has either to correct the data to the parton level or "dress" the theory with fragmentation effects.

In the first case the question is : Which parton level? It has been suggested by Kunszt and Nason[59] that one should use the parton shower parton level, since the averaged number of partons with invariant masses above 1 GeV between all pairs is about 11 at LEP energies, which is significantly higher than the maximum number of 4 partons in second order QCD. However, comparing this LLA parton level with an exact second order QCD calculation with at most two gluons is inconsistent and does not lead to a determination of $\Lambda_{\overline{MS}}^{(5)}$ in second order, but rather to a scale which is a mixture of the LLA and exact second order QCD. For convenience I call this scale Λ_{LL2}.

As mentioned before, most of the additional gluons in the LLA are soft and the jet rates can be well described in second order too. Therefore, one can use the second order ME for extracting α_s from the jet rates, especially since these are rather insensitive to the fragmentation parameters and the exact tuning of the distributions within a jet.

The results of the two methods can be rather different, as is demonstrated in Fig. 17, which compares the jet rates for the parton shower- and matrix element models. If one inserts Λ_{LL2} into the second order Monte Carlo, one finds

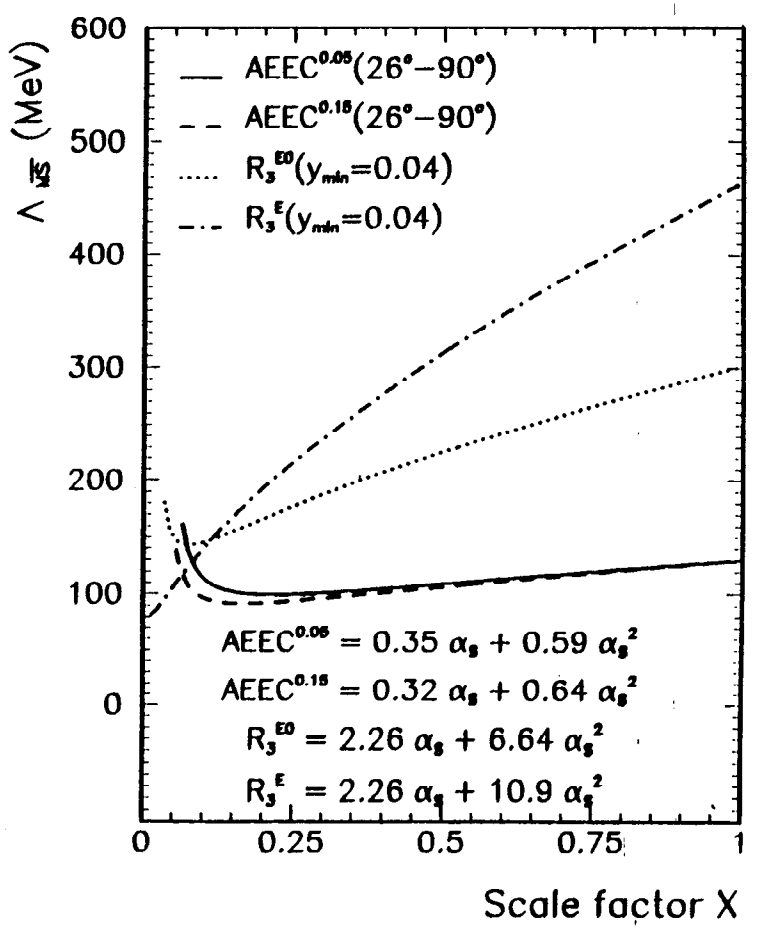

Figure 16: The renormalization scale dependence of $\Lambda_{\overline{MS}}^{(5)}$ for the AEEC and the 3-jet rate R_3. R_3^{E0} and R_3^{E} are the 3-jet rates for the $E0$ and E recombination schemes. The upper index of the AEEC indicates the energy cut in the Sterman-Weinberg recombination scheme.

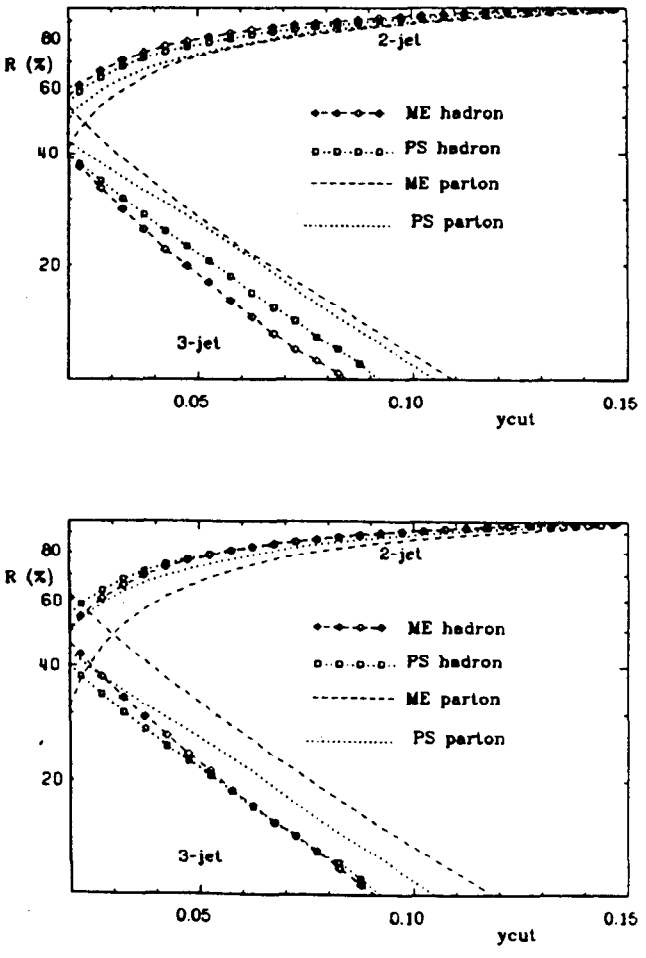

Figure 17: A comparison of the jet rates at the parton- and hadron level for the matrix element (ME) and parton shower (PS) models for the scale Λ_{LL_2}=154 MeV (a) and $\Lambda^{(5)}_{\overline{MS}}$=350 MeV (b). In case (a) one fits the parton levels to each other, in case (b) the hadron levels. Clearly, these two fitting procedures do not yield the same Λ for this variable.

indeed that the parton levels agree[3], as expected, since this was how Λ_{LL_2} has been determined, but at the hadron level the 3-jet rate is clearly too low for the second order ME[4]. The scale $\Lambda^{(5)}_{\overline{MS}}$ has to be increased to 350 MeV in order to get agreement at the hadron level (see Fig. 17b), which clearly shows that $\Lambda^{(5)}_{\overline{MS}}$ is different from Λ_{LL_2} in this case. Therefore, fitting a second order expression for the 3-jet rate to the data, corrected to the parton level of the parton shower model, does not necessarily lead to a consistent determination of $\Lambda^{(5)}_{\overline{MS}}$ in the sense that putting Λ_{LL_2} into a second order Monte Carlo does not reproduce the jet rates.

Fortunately, there is no need to use such inconsistent methods, since the number of events with more than two hard gluons ($\propto \alpha_s^3$) is negligible, even at LEP energies and the ME models can describe the data well in the regions where hard gluon radiation is important.

'Good' variables to determine α_s are those who show a large sensitivity to $\Lambda^{(5)}_{\overline{MS}}$ and a small sensitivity to the fragmentation parameters. If α_s is determined by asking which $\Lambda^{(5)}_{\overline{MS}}$ in the Monte Carlo gives the best description of the data, one does not worry so much about the close correspondence between partons and hadrons, as long as the difference between them is well described by the Monte Carlo and rather insensitive to the tuning of the fragmentation parameters. For example, for the AEEC the fragmentation effects are non-neglibible, but well described by the Monte Carlo and insensitive to the tuning of the fragmentation parameters (see Sect. 8).

7.3 Recombination Scheme Dependence

A definition of the jet multiplicity requires the definition of a jet resolution and a 'jet finder' algorithm. The most popular jet finders have been the ones based on invariant masses: the four vectors of the two particles or 'pseudo-particles' are added to form a new pseudo-particle. This process is repeated until the scaled invariant mass $y = M^2_{ij}/s$ between all pairs of pseudo-particles are above a certain minimum value y_{min}. The number of pseudo-particles is by definition the jet multiplicity.

There are several ways to add the particles to pseudo-particles[59,53]. The most common ones have been summarized in Table 3. In all cases the direction of a pseudo-particle is determined by the vectorial sum of the 3-momenta of the two primary particles. The schemes differ in the calculation of the energy and the invariant masses. In the so-called P-schemes the pseudo-particles are kept massless by setting the energy equal to the momentum, thus resembling massless partons, which is convenient for Monte Carlo applications. However, this does not conserve energy; in the P0-scheme y_{cut} is rescaled to the continuously decreasing energy. The E-scheme is Lorentz invariant, so it can be applied in any reference frame; the others have to be applied in the laboratory frame. In most schemes

[3]Here I used Λ_{LL_2}=154 MeV for an 'optimum' renormalization scale factor f=0.113, as determined by OPAL[53].

[4]The comparison was only made for the ERT ME with the P-recombination scheme, since this is the one which is available as default in the JETSET 7.2 Monte Carlo.

Schemes	M_{ij}^2	p_{ij}	Remarks
E	$(p_i + p_j)^2$	$p_{ij} = p_i + p_j$	Lorentz invariant
JADE	$2E_iE_j(1 - \cos\theta_{ij})$	$p_{ij} = p_i + p_j$	masses neglected in M_{ij}
E0	$(p_i + p_j)^2$	$\vec{p}_{ij} = \frac{E_{ij}}{\lvert\vec{p}_i+\vec{p}_j\rvert}(\vec{p}_i + \vec{p}_j)$ $E_{ij} = E_i + E_j$	$\vec{p}$ not conserved
P	$(p_i + p_j)^2$	$\vec{p}_{ij} = \vec{p}_i + \vec{p}_j$ $E_{ij} = \lvert p_{ij}\rvert$	E not conserved
P0	as P	as P	as P, but y_{cut} rescaled to new E_{ij} after each recombination

Table 3: Jet Recombination Schemes. The index ij indicates components of the pseudo-particle built from the particles i and j.

y=0.02	*JADE scheme*			*P scheme*			*P0 scheme*			*E scheme*		
	2-j	3-j	4-j	2-j	3-j	4-j	2-j	3-j	4-j	2-j	3-j	4-j
2-p	0.29	0.10	0.00	0.34	0.05	0.00	0.33	0.05	0.00	0.06	0.27	0.04
3-p	0.14	0.35	0.04	0.18	0.32	0.02	0.17	0.33	0.02	0.01	0.29	0.21
4-p	0.00	0.04	0.05	0.01	0.05	0.04	0.00	0.04	0.05	0.00	0.01	0.06

y=0.05	*JADE scheme*			*P scheme*			*P0 scheme*			*E scheme*		
	2-j	3-j	4-j	2-j	3-j	4-j	2-j	3-j	4-j	2-j	3-j	4-j
2-p	0.64	0.06	0.00	0.68	0.02	0.00	0.67	0.03	0.00	0.40	0.27	0.00
3-p	0.08	0.21	0.00	0.11	0.17	0.00	0.10	0.19	0.00	0.03	0.25	0.04
4-p	0.00	0.01	0.01	0.00	0.01	0.01	0.00	0.01	0.01	0.00	0.00	0.01

y=0.08	*JADE scheme*			*P scheme*			*P0 scheme*			*E scheme*		
	2-j	3-j	4-j	2-j	3-j	4-j	2-j	3-j	4-j	2-j	3-j	4-j
2-p	0.78	0.04	0.00	0.81	0.01	0.00	0.80	0.02	0.00	0.63	0.16	0.00
3-p	0.06	0.13	0.00	0.07	0.10	0.00	0.06	0.11	0.00	0.03	0.17	0.01
4-p	0.00	0.00	0.00	0.00	0.00	0.00	0.00	0.00	0.00	0.00	0.00	0.00

Table 4: The transition probabilities of parton multiplicities (n-p) to hadron jet multiplicities (n-j) at 91 GeV in the various recombination schemes for a jet resolution y of 0.02, 0.05, and 0.08, respectively. Here I have used the standard ERT matrix element as implemented in JETSET 7.2 and applied the same cluster algorithm to the parton and hadron level. The probabilities have been normalized to the total number of events, so the sum is one and the sum within each column yields the n-jet rate at the hadron level, while the sum within each row yields the n-jet rate at the parton level. Note that for the 'JADE' scheme the 2-p to 3-j transition is approximately equal to the 3-p to 2-j transition, which results in approximately equal jet rates at the hadron- and parton level, although the migration between the 2- and 3-jet classes is as large as 30% .

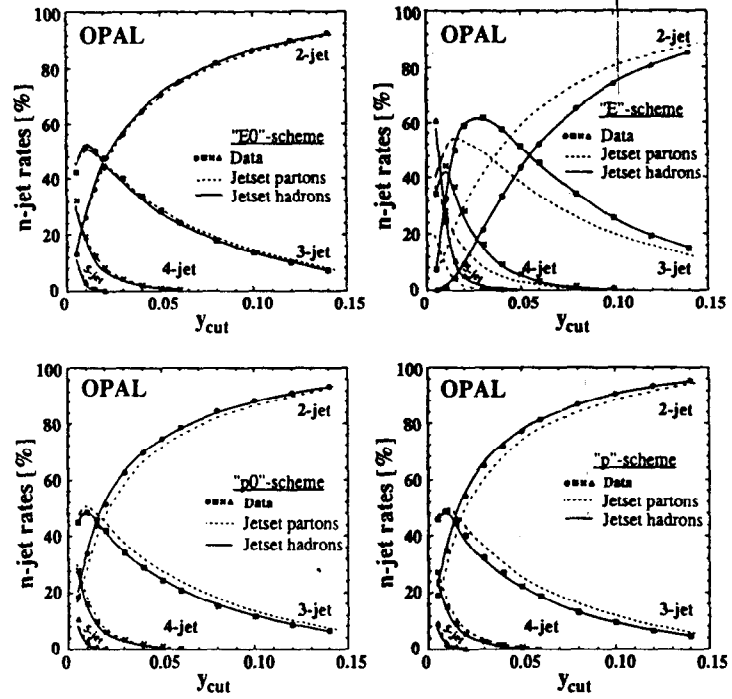

Figure 18: The fractional jet multiplicities as function of the jet resolution for 4 recombination schemes at the hadron - and parton level for the Lund parton shower model. Data from OPAL.

the invariant mass is calculated exactly, i.e.,

$$M_{ij}^2 = p_i + p_j = 2E_iE_j(1 - cos\theta_{ij})) + m_i^2 + m_j^2 \ .$$

In the JADE scheme the masses m_i and m_j are put to zero. In practice the E0 scheme is close to the JADE scheme[53]. The JADE jetfinder has become so popular, while the jet rates at the hadron level are close to the jet rates at the parton level in contrast to the other recombinations schemes. This is shown in Fig. 18 from a study by OPAL, who compare the jet multiplicities as function of the jet resolution at the hadron and parton level[49,53] using the parton shower Monte Carlo JETSET 7.2. One observes good agreement with the data for all recombination schemes for a single value of the QCD scale in the Monte Carlo. This recombination scheme independence is only possible for small renormalization scales, in which case all methods tend to yield similar $\Lambda_{\overline{MS}}^{(5)}$ values (see Fig. 16).

The correspondence between a 3-jet event at the parton - and hadron level is not one to one, even for the JADE scheme, as suggested by Fig. 18. For example, if one generates only 3-parton events in the Monte Carlo, about 30 % of them

become 2-jet events at the hadron level, as shown in Table 4. On the other hand 2-jet parton events contribute to the 3-jet rate at the hadron level and the average number of 3-jet events at parton and hadron level happen to agree very well, but this is purely accidental. Therefore, it is not a priori clear if the JADE-scheme is a much better scheme than the others for the determination of α_s.

From Table 4 one observes too, that the large 'fragmentation correction' in the E-scheme, i.e., the difference in jet rates between hadron- and parton level, originates from the large background of 2-jet events, which become classified as 3-jet events because of the large jetmasses at the hadron level, while the large 'fragmentation correction' in the P-schemes is due to the purity of the 3-jet sample, i.e., the background from 2-parton states is small and does not compensate the losses of the migration of 3-p to 2-j like in the JADE scheme. Note too that the purity of the 4-jet sample is highest in the P-schemes, i.e., the background from 3-p events is small.

The extraction of α_s from the data has been done in rather different ways by the different groups:

The OPAL Collaboration follows the suggestion by Kunszt and Nason and correct their data to the parton level in the PS model, using all possible recombination schemes given in Table 3.

DELPHI, L3 and MARK-II analyze their data, shown in Fig. 19, within the framework of second order QDC. MARK-II uses only the E0-scheme, in which the fragmentation corrections are small (3-5%). They neglect this correction and fit the parton level expression directly to the data, but include this missing correction in the systematic error. DELPHI and L3 correct the theoretical jet rates with a correction matrix in order to be able to compare them directly to the data. The DELPHI Collaboration has obtained this matrix from the exact second order ME Monte Carlo, based on the KL' matrix element[61]. They noted that for the KL' scheme this matrix correction is very small and used it for the other recombination schemes too. The L3 Coll aboration has used the GKS matrix element[26], which is the default in the JETSET 7.2 Monte Carlo.

The final results from DELPHI[50], L3[51] OPAL[49,53], and MARK-II[52] have been summarized in Table 5. In all cases the $\Lambda^{(5)}_{\overline{MS}}$ have been determined from a fit of the theoretical expressions[61,59] of the form:

$$\begin{aligned} R_2 &\equiv \frac{\sigma_2}{\sigma_{tot}} = 1 + C_{2,1}\cdot\alpha_s + C_{2,2}\cdot\alpha_s^2 \\ R_3 &\equiv \frac{\sigma_3}{\sigma_{tot}} = C_{3,1}\cdot\alpha_s + C_{3,2}\cdot\alpha_s^2 \\ R_4 &\equiv \frac{\sigma_3}{\sigma_{tot}} = C_{4,2}\cdot\alpha_s^2 \end{aligned} \qquad (6)$$

where σ_{tot} is the total hadronic cross section and σ_n are the corresponding n-parton cross section. $C_{n,k}$ are the k - th order QCD coefficients for n - parton events.

Some care has to be taken in fitting the jet rates as function of the jet resolution because of correlations: a single event can contribute to all jet classes simultaneously, of course for different jet resolutions. To avoid such correlations the L3 Collaboration has taken the sensible approach of fitting R_3 for only one

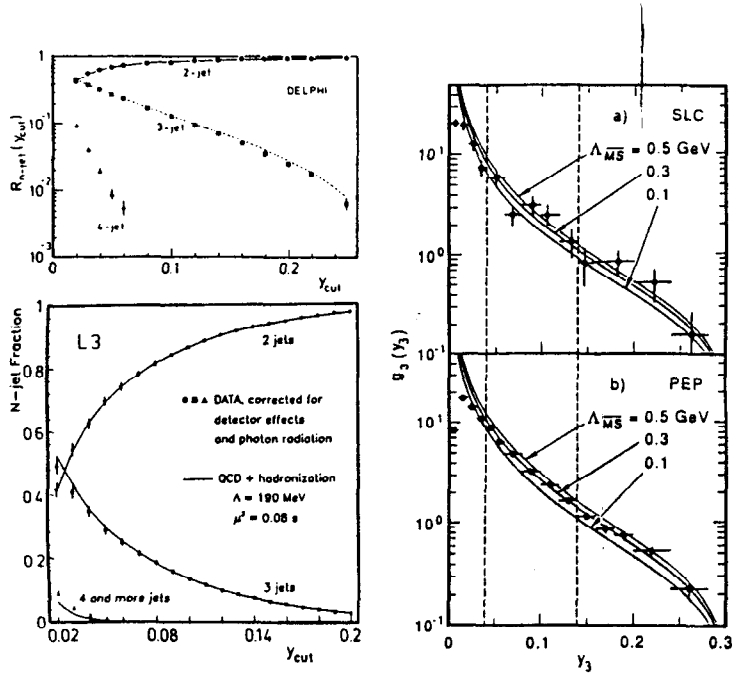

Figure 19: The fractional jet rates as function of the jet resolution from DELPHI and L3 and the y_3 distribution from MARK-II at 29 and 91 GeV. y_3 is defined as the smallest invariant mass in the events, reconstructed as 3-jet events. Note that the curves through the DELPHI data use an 'optimized' scale, which yields a good description of the 4-jet rate.

value of the jetresolution -y_{cut} = 0.08- and considers the comparison of the jet-rates for other y_{cut} values as test of QCD. Such a selection of jets increases the statistical error somewhat, but this error is anyway negligible compared to the systematic errors. The other collaborations have fitted the differential jet rates, in which each event enters only once in the transition from jet i+1 to jet i.

In spite of all the differences in analyzing the data, the results of the groups agree within errors, but these errors are large and dominated by the renormalization scale dependence of the various schemes, as shown in Table 5 and expected from Fig. 16. It should be noted that some experiments have quoted the α_s value symmetrized between the one for a renormalization scale factor $f = 1$ and f small, others only quote the value for $f = 1$. Figure 20 shows the α_s values for the small scale $f \approx 0.002$ and $f = 1$ separately, which clearly shows that the renormalization scale dependence is the dominating error.

The arrow on the values for $f = 1$ indicates that this f value is a rather

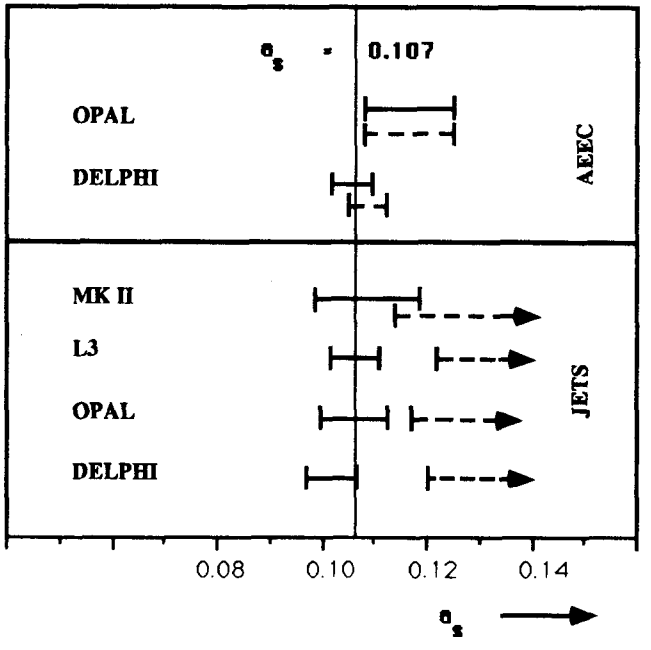

Figure 20: A summary of α_s values from jet multiplicities (JADE recombination scheme) and the asymmetry in energy energy correlations. The solid lines correspond to the values obtained for an optimized renormalization scale, while the dashed lines correspond to $Q^2 = s$. For the AEEC the two values are close together, while for the jetmultiplicities the scale dependence is the dominating error. The vertical line at α_s=0.107 corresponds to the averaged value of the solid lines.

arbitratry cutoff. Theoretically there is no strong reason why one should not consider the errors from even larger scales, since, as mentioned before, physical observables are independent of the choice of scale, if the higher order contributions are negligible. As is obvious from Fig. 16, larger values would lead to larger values of α_s.

It should be noted that for the fragmentation corrections in all cases Monte Carlos with a small scale have been used, since only in this case the contributions from four or more jets have been estimated correctly. Therefore, it is more consistent to quote the α_s values corresponding to the small scales. Averaging the values for the small scales (including the one for the AEEC, to be discussed in the next section) leads to

$$\alpha_s = 0.107 \pm 0.007,$$

as indicated by the vertical line Since the errors are dominated by systematics, it is difficult to estimate the error. As a conservative estimate I have taken half

Exp.	α_s	(*exp. err.*)	(*theor. err.*)
DELPHI	0.114	± 0.005	± 0.012
OPAL	0.116	± 0.006	± 0.008
L3	0.115	± 0.005	$^{+0.012}_{-0.010}$
MARK – II	0.123	± 0.010	$^{+0.000}_{-0.014}$

Table 5: $\alpha_s(M_Z^2)$ from jet rates. The theoretical error is dominated by the variation of the renormalization scale factor f between 0.001 and 1.

of the difference between the two extreme values.

Recently, the recombination dependence has been studied by Kramer and Magnussen[62]. They find little difference between the E- and E0-scheme in contrast to the results from OPAL[53] and the numbers in Table 4. This appears to be due to the fact that they apply the E0 invariant mass criteria to the pseudo-particles from the E-scheme, so there E-scheme is really E*E0 and it is not surprising that these two agree, since now the clustering as well as the jet resolution criteria are similar.

8 Energy-Energy Correlations

The asymmetry in the energy-energy correlation (AEEC) was introduced by Basham, Brown, Ellis and Love[63] as a 'good' observable to determine the strong coupling constant α_s, since it is relatively insensitive to fragmentation effects, which mainly contribute symmetrically to the energy-energy correlations (EEC). Subsequently the second order corrections have been calculated[60,64,65,59], and found to be reasonably small at the parton level (15% for the AEEC at the parton level). Experimentally the energy–energy correlation (EEC) can be defined as a histogram of all angles between all pairs of particles, weighted with their energies:

$$\mathrm{EEC}(\chi) = \frac{2}{N}\sum_{events}^{N}\sum_{i}^{N_{par}-1}\sum_{j>i}^{N_{par}}\frac{E_i E_j}{E_{vis}^2}\cdot\left(\frac{1}{\Delta\chi}\int_{\chi-\frac{\Delta\chi}{2}}^{\chi+\frac{\Delta\chi}{2}}\delta(\chi'-\chi_{ij})d\chi'\right)$$

where E_i is the energy of particle i, χ_{ij} is the angle between particles i and j, χ is the opening angle for which one studies the correlation, $\Delta\chi$ is the bin width, N is the number of events, N_{par} is the number of particles in the event, and the

Exp.	$\alpha_s(M_Z^2)$	Λ
DELPHI	$0.106 \pm 0.004[exp.]^{+0.003}_{-0.000}[theor.]$	$\Lambda^{(5)}_{\overline{MS}} = 104\ ^{+35}_{-28}[exp.]^{+30}_{-00}[theor.]$
OPAL	$0.117^{+0.007}_{-0.009}[exp.]^{+0.006}_{-0.002}[theor.]$	$\Lambda_{LL2} = 211^{+92}_{-92}[exp.]^{+75}_{-20}[theor.]$

Table 6: α_s from the asymmetry in the energy-energy correlations.

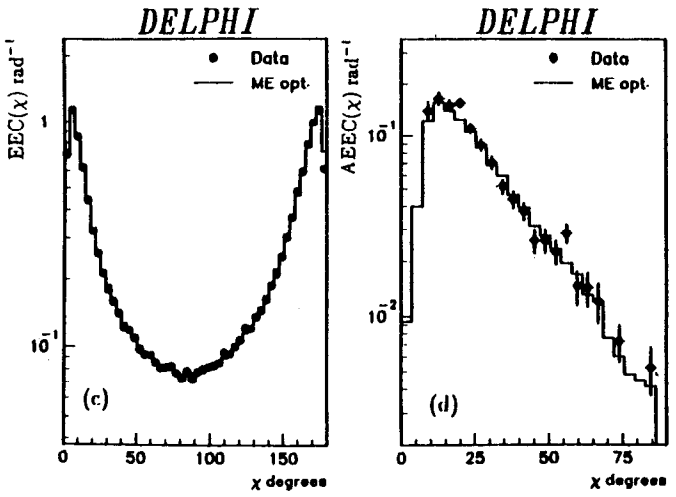

Figure 21: The corrected EEC and AEEC at the hadron level compared with the exact second order QCD matrix element Monte Carlo followed by string fragmentation. Data from DELPHI.

weights are normalized to the visible energy $E_{vis} = \sum_i^{N_{par}} E_i$. The integral of the δ-function is 1 for combinations inside the bin and zero otherwise.

Such a histogram shows two peaks (see Fig. 21): the peak below 30° corresponds to the angles between pairs of particles inside a jet, while the peak near 180° corresponds to angles between particles in opposite jets. Gluon radiation causes an asymmetry around 90°. This can be seen easily at the parton level, where two large angles and one small angle in a $q\bar{q}g$ event give more entries at large angles than at small angles.

The asymmetry is defined as:

$$\mathrm{AEEC}(\chi) = \mathrm{EEC}(180° - \chi) - \mathrm{EEC}(\chi), \quad 0° < \chi \leq 90° \ .$$

On average, the 2-jet contribution to the EEC cancels in the asymmetry. This is a unique feature of the asymmetry: it is rather insensitive to the tuning of the fragmentation parameters, which mainly change the EEC in a symmetric way. The weighting of the angles with the energy makes the EEC infrared stable, i.e., the contribution of soft gluons goes to zero as their energy goes to zero.

Many experiments have studied the AEEC and determined α_s[66]. At LEP the AEEC has been studied by the DELPHI- and OPAL Collaborations[67,68]. The resulting α_s values have been summarized in Table 6 and plotted together with the α_s values from the jet rates in Fig. 20. The approaches from OPAL and DELPHI differ like in the α_s determinations from the jet rates: OPAL corrects to the parton level of the parton shower program and fits various second order

.....CLASSES.....	WEIGHTS	QCD	ABEL.	TOYMOD.
A 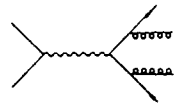	C_F^2	34%	27%	90%
B	$C_F(C_F - N_C/2)$	−5%	32%	
C 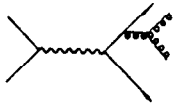	$C_F N_C$	65%	0%	0%
D 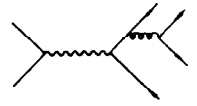	$C_F T_R$	6%	41%	10%
E	$C_F(C_F - N_C/2)$	−0.1%	0.5%	

Table 7: Contributions to 4-jet events in second order QCD and theories without gluon self coupling. The last three colums give the fraction in each class after the DELPHI detector simulation.

expressions to this parton level of the LLA combined with the first order matrix element, thus determining Λ_{LL2} as defined in the previous section. Their quoted experimental error is dominated by the difference between the analysis based on charged and neutral tracks, while the theoretical error stems from the difference between the various second order QCD calculations. The given α_s value is for a renormalization scale of f=1, but they find the dependence on the scale to be negligible.

DELPHI has determined α_s within the framework of exact second order QCD by fitting the $\Lambda^{(5)}_{\overline{MS}}$ in the JETSET 7.2 Monte Carlo using the ERT matrix element. Their quoted errors have similar contributions from statistical and systematic errors. The latter have been estimated by varying the fragmentation parameters of the longitudinal- and transverse fragmentation function, which are the main ones influencing the angles of the leading particles (remember the AEEC is weighted with the energy of the particles). The quoted value is for a renormalization scale f=0.002, which is the default value in the Monte Carlo and is known to give a correct description for the contribution of the 4-jet rate. If the scale in the Monte Carlo is set to 1, they find that $\Lambda^{(5)}_{\overline{MS}}$ increases by 30 MeV, which is quoted as the theoretical error. As is clear from Fig. 20, the α_s values from the jetmultiplicities and AEEC are in excellent agreement with each other. The fact that these methods with completely different contributions from fragmentation yield the same value of α_s gives confidence in our understanding of the event structure originating from perturbative QCD.

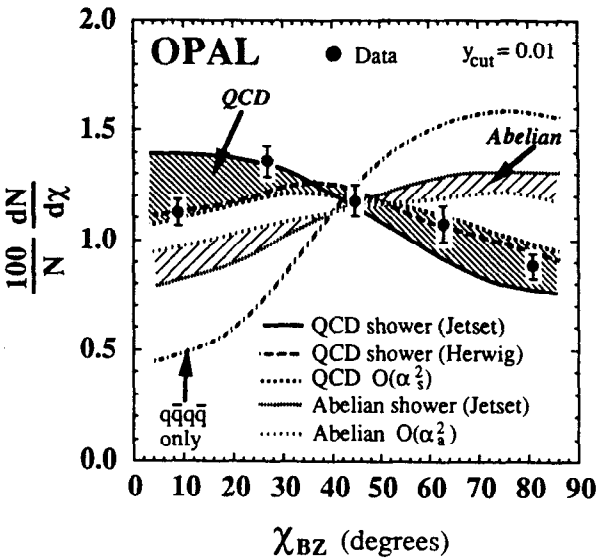

Figure 22: **Distribution of χ_{BZ} in 4-jet events with $y_{cut} = 0.01$ compared with QCD, the abelian theory and $q\bar{q}q\bar{q}$ only. The difference between the abelian theory and QCD stems mainly from the difference in 4-quark final states, not from the absence of the triple gluon vertex in the abelian theory. Data from OPAL.**

9 Search for Triple Gluon Vertex

In QCD the gluons carry colour, which implies that gluons can interact between themselves. This gluon self interaction is responsible for the running of the coupling constant, as discussed before and thought to be responsible for the confinement of quarks inside hadrons. However, it is difficult to prove the existence of the gluon self interaction directly. In high energy proton-proton collisions the 2-jet cross sections would be much smaller without gluon-gluon interactions.

In e^+e^- annihilation the triple gluon vertex leads to additional 4-jet final states ($q\bar{q}gg$). However, double gluon bremsstrahlung and four quark final states lead to 4-jet final states too and distinguishing between all three contributions by means of the different angular correlations due to the different helicities in the final state is not easy. Table 7 summarizes the contributions from the various classes in QCD and the Abelian analog, in which the triple gluon vertex has been put to zero. These contributions are only approximate, since mass effects have not been included. Note furthermore, that each class has many more graphs contributing than indicated by the graphs in quotes, since these single graphs are not gauge invariant. Only the groups of classes proportional to specific group constants are gauge invariant. However, all the graphs within e.g., class C would be zero, without this 'main' graph, in this case the triple gluon vertex.

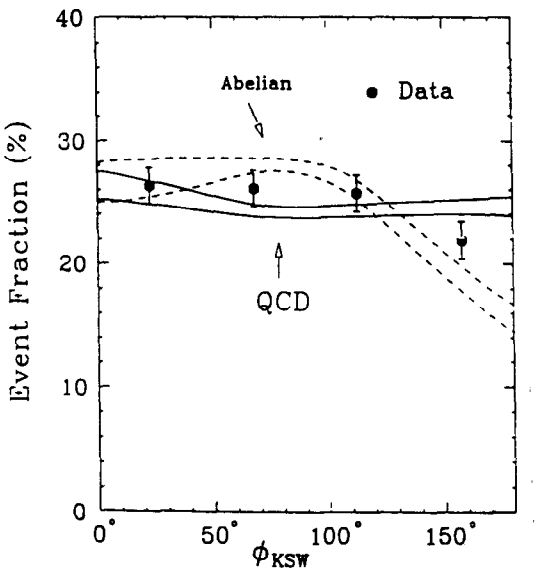

Figure 23: **Distribution of ϕ_{KSW} in 4-jet events with $y_{cut} = 0.02$ compared with QCD and the abelian theory. Data from L3.**

One observes, that the Abelian theory has a considerably larger fraction of 4-quark final states and it turns out that the angles proposed by Körner et al.[69], Bengtsson and Zerwas[70], and Nachtman and Reiter[71] are rather sensitive to this fraction[72,73,74]. Therefore, from a comparison of these angles with the data several experiments have been able to exclude the Abelian theories[75,74,76,77,78]. Recent results from the L3- and OPAL Collaborations are shown in Figs. 22 and 23[76,77].

However, these angles cannot distinguish very well between the $q\bar{q}gg$ contributions from *double Bremsstrahlung* and *triple gluon vertex*, so excluding the Abelian theories by the angles mentioned above is still no direct proof for the gluon self interaction. One could just replace the contributions from the triple gluon vertex with *more* double Bremsstrahlung to get the same angular distributions. For example, such a 'toy model' in Table 7 yields about the same distributions for the angles mentioned above. However, it turns out that the gluons from double bremsstrahlung contributions have a larger averaged opening angle than the gluons from triple gluon graphs[73], as shown in Fig. 24. If one fits simultaneously the opening angle α_{ij} between the two least energetic jets in 4-jet events and the generalized Nachtman-Reiter angle θ^*_{NR}[79], one can distinguish between *all* 4-jet contributions: θ^*_{NR} forbids a too large $q\bar{q}q\bar{q}$ contribution, so $q\bar{q}gg$ is needed, but α_{ij} restricts the contribution from double bremsstrahlung (mainly class A) so part of it must come from the triple gluon vertex graphs (class C).

The DELPHI Collaboration[78] has made a preliminary study of the 2-dimensional distribution in θ^*_{NR} and α_{ij}. As free parameters they have taken the ratio

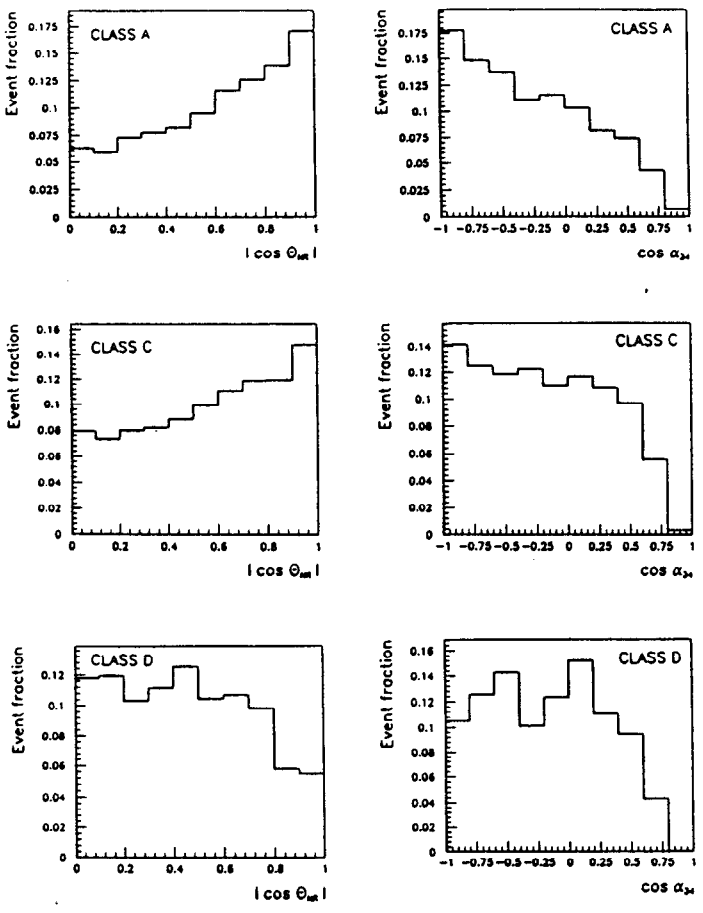

Figure 24: Distribution of generalized Nachtmann-Reiter angle θ^*_{NR} and opening angles between the two least energetic jets (α_{ij}) for double Bremsstrahlung- (class A), triple gluon vertex- (class C), and $q\bar{q}q\bar{q}$ graphs (class D). Classes A and C can be distinguished from class D by θ^*_{NR}, while class C can be separated from class A by α_{ij}. The contributions from classes B and E are small.

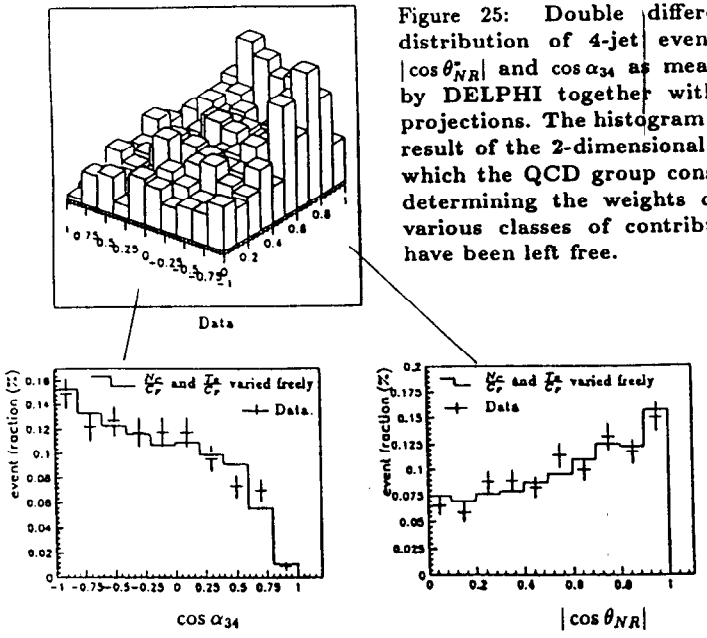

Figure 25: Double differential distribution of 4-jet events in $|\cos\theta^*_{NR}|$ and $\cos\alpha_{34}$ as measured by DELPHI together with the projections. The histogram is the result of the 2-dimensional fit in which the QCD group constants determining the weights of the various classes of contributions have been left free.

of N_C/C_F and T_R/C_F, which are the group constants determining the weights in front of the various classes shown in Table 7. From theory one expects:

$$C_F = 4/3, N_C = 3, T_R = n_f/2 \text{ for QCD}$$

$$C_F = 1, N_C = 0, T_R = 15 \text{ for ABELIAN}$$

From a sample of 21000 Z^0's, they selected with the LUCLUS jetfinder[20] a sample of 884 4-jet events. From the fit they find:

$$N_C/C_F = 2.05 \pm 0.4[stat.]^{+0.8}_{-0.4}[syst.]$$

$$T_R/C_F = 0.1 \pm 1.7$$

In QCD the class of diagrams containing the triple gluon vertex graphs (class C) is proportional to N_C/C_F, so a non-zero value gives direct evidence for the triple gluon vertex without reference to a specific model. The observed value for this ratio is in good agreement with the value expected in QCD (2.25), although the errors are still large: the first error is the statistical error, the second one originates from the uncertainties from fragmentation models and the fitting procedure.

10 Conclusion

After one year of LEP running the harvest in the QCD area has been rewarding, not only because of the large number of events, but also because of the quality

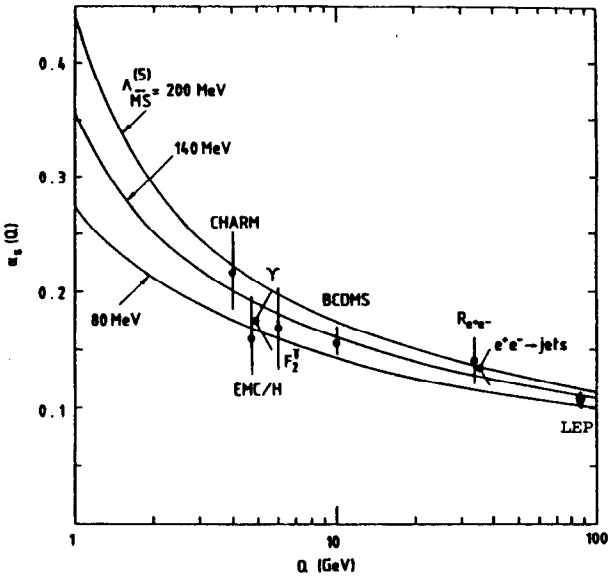

Figure 26: The α_s values from various reactions.

of the events: a sizable fraction ($\approx$ 20%) are 3-jet events with an average gluon energy of 20 GeV, while about 5% of the events are clean 4-jet events, in which the least energetic jet still has typically a total energy of 20 GeV. These 'healthy' gluon jets combined with 'state of the art' Monte Carlo models provided QCD tests with unprecedented quality.

Among the results:

- All hadronic decays from the Z^0 are amazingly well described by parton shower models tuned at lower energies. Especially the intermittency studies find excellent agreement between data and Monte Carlo, indicating that the origin of the strong intermittency observed in e^+e^- annihilation does not need new physics contrary to previous expectations. The charged multiplicities turn out to be both in agreement with KNO scaling and the predictions of the parton shower models.

- The models based on the exact second order QCD matrix element needed retuning at 91 GeV, mainly because the Q^2 evolution of the fragmentation functions have not been included. After retuning the parameters these models could be brought into reasonable agreement with the parton shower model, at least in the regions where the hard gluons dominate. Especially, all jet rates agree remarkably well, provided a similar definition of the coupling constant is used, i.e., the scale of α_s in the ME models is chosen to be of the order of a few GeV, like in the PS model, where the scale is chosen to be of the order of the p_t of the gluon. The second order ME Monte Carlo model allows quantitative studies without the approximations inherent in the parton shower model.

- The new determinations of the strong coupling constant are in excellent agreement with the predictions from $\Lambda^{(5)}_{\overline{MS}}$ measurements at lower energies as shown in Fig. 26 (from Ref. [80]). It should be noted that this plot is *no* evidence for the running of α_s, since the value from LEP might just as well have been plotted at the optimized scale of a few GeV, as used in the programs. The lines indicate the α_s dependence for constant values of $\Lambda^{(5)}_{\overline{MS}}$. Note that the range of $\Lambda^{(5)}_{\overline{MS}}$ values lead to very small errors in α_s at high energies. Plotting the LEP data at lower scales increases not only the absolute errors, but the relative errors too!

- Evidence for the running of α_s can be best obtained by the Q^2 dependence of a single observable and the new data on the 3-jet rate combined with the data at PEP and PETRA give enough lever arm in Q^2 to provide direct evidence for the running of α_s.

- The angular correlations in 4-jet events provide a sensitive test of the spin and colour structure of QCD. The Abelian type theories are excluded, while first evidence for the triple gluon vertex starts to emerge.

11 Acknowledgment

Writing a review about so many new and interesting data cannot be done without the help of many experts. Here I want to thank all of those, who have been willing to share their experience and ideas and make available preliminary data before publication.

Especially, I want to thank Siggi Bethke, Thomas Hebbeker, Sachio Komamiya, Zoltan Kunszt, Peter Mättig, Paolo Nason, and Torbjorn Sjöstrand for interesting discussions and last, but not least I wish to thank my colleagues within DELPHI for many discussions, friendship, and such a joyful collaboration.

References

[1] A. Bialas and R. Peschanski, Nucl. Phys. **B273** (1986) 703, ibid. **B308** (1988) 857.

[2] R.C. Hwa, Phys. Lett. **B201** (1988) 165, OITS-385 (1988).

[3] I.M. Dremin, JETP Lett. **30** (1980) 152,
Sov. J. Nucl. Phys. **33** (1981) 726.

[4] J. Dias de Deus, Phys. Lett. **B194** (1987) 297.

[5] W. Ochs, J. Wosiek, Phys. Lett. **B214** (1988) 617.

[6] A. Bialas (CERN), CERN-TH-5791-90, Jul 1990. 25pp.
A. de Angelis, to be published in Mod. Phys. Lett. A
G. Gustafson, A. Nilsson, LU-TP-90-7, May 1990.
J. Dias de Deus, IFM-16/89, Multiparticle Dynamics, (Festschrift for Leon Van Hove), World Scientific, A. Giovannini and W. Kittel (Eds.), Singapore, 1990.
B. Buschbeck, P. Lipa, Mod. Phys. Lett. A4 (1989) 1871.
W. Kittel and R. Peschanski, HEN-325
H. Satz, CERN-TH-5589/89
P. Carruthers, H.C. Eggers, Ina Sarcevic, AZPH-TH-90-46
Hadronic multiparticle production, P. Carruthers, (Ed.) 1988.
L. Van Hove and A. Giovannini, CERN-TH-4957/88, Acta Phys. Polon. **B19** (1988) 931
Further excellent reviews were given at the Int. Workshop on Intermittency in High Energy Collisions, Santa Fe, NM, Mar 18-21, 1990 by
R. C. Hwa, OITS-440, Apr 1990.
W. Ochs, MPI-PAE-PTH-35-90
I. Sarcevic, AZPH-TH-90-42 and AZPH-TH-90-43
K. Sugano, ANL-HEP-CP-90-37.

[7] DELPHI Collaboration, P. Abreu, et al., CERN-EP/90-78, subm. to Phys.Lett.B.

[8] TASSO Collab., Phys. Lett. **B231** (1989) 548.

[9] CELLO Collab., H. J. Behrend et al., to be published
M. Feindt, talk at the Int. Conf. on High Energy Phys., Singapore, 1990
O. Podobrin, talk at the XX. Int. Symposium on Multipart. Dyn., Dortmund, 1990.

[10] HRS Collab., S. Abachi, et al., ANL-HEP-CP-90-50
By K. Sugano, ANL-HEP-CP-90-37 and invited talk at the Int. Conf. on High Energy Phys., Singapore, 1990.

[11] QCD generators for LEP, Study group convenor: T. Sjöstrand, published in Proc. of the 1989 Workshop on Z Physics at LEP 1, B. Bambah et al., CERN 89-08, Vol. 3, p.143, Eds. G. Altarelli, R. Kleiss and C. Verzegnassi.

[12] E.D. Malaza, B.R. Webber, Nucl. Phys. **B267** (1986) 702; Phys. Lett. **149B** (1984) 501.

[13] Z. Koba, H.B. Nielsen and P. Olesen, Nucl. Phys. **B40** (1972) 317
The scaling behaviour of the multiplicity in e^+e^- annihilation was already given by A.M. Polyakov, Sov. Phys. JETP **32** (1971) 296, ibid. **33** (1971) 850.

[14] J. Drees, DELPHI Note 90-41 Phys 68, Invited talk at the 14th Int. Conf. on Neutrino Phys. and Astrophys., Geneva (1990).

[15] MARK-II Collab., G.S. Abrams, et al., Phys. Rev. Lett. **64** (1990) 1334.

[16] ALEPH Collab., D. Decamp et al., Phys. Lett. **B234** (1990) 209
An update on $< N_{ch} >$ was given by M. Schmelling, ALEPH 90-123 PHYS 74, to appear in the Proc. of the Renc. de Moriond, (1990).

[17] DELPHI Collab., P.Aarnio et al., Phys. Lett. **B240** (1990) 271.

[18] DELPHI Collab., P. Abreu, et al., CERN-EP/90-117, updated version, subm. to Z. Phys.

[19] OPAL Collab., M.Z. Akrawy, et al., CERN-EP/90-48.

[20] T. Sjöstrand, Comp. Phys. Comm. **27** (1982) 243, ibid. **28** (1983) 229
T. Sjöstrand and M. Bengtsson, Comp. Phys. Commun. **43** (1987) 367.

[21] G. Marchesini and B.R. Webber, Nucl. Phys. **B310** (1988) 464; Herwig version 4.3.

[22] R. Szwed and G. Wrochna, Z. Phys. **C47** (1990) 449.

[23] J. Ellis, M. Karliner, H. Kowalski, Phys. Lett. **B235** (1990) 341.

[24] OPAL Collab., M.Z. Akrawy, et al., CERN-EP/90-55.

[25] J. Ellis, M.K. Gaillard, and G.G. Ross, Nucl. Phys. **B111** (1976) 253; ibid. **B130** (1977) 516
A. Ali et al., Nucl. Phys. **B167** (1980) 454; Phys. Lett. **82B** (1979) 285
J.G. Körner et al., Nucl. Phys. **B185** (1981) 365
K.J.F. Gaemers and J.A.M. Vermaseren, Z. Phys. **C7** (1980) 81
O. Nachtmann and A. Reiter, Z. Phys. **C14** (1982) 47; ibid. **C16** (1982) 45
Z. Kunszt, Phys. Lett. **99B** (1981) 429
A. Ali and B. Barreiro, Nucl. Phys. **B236** (1984) 269
R.-Y. Zhu, MIT Ph. D. thesis (1984)
F. Gutbrod, G. Kramer, G. Schierholz, Z. Phys. **C21** (1984) 235
F. Fabricius et al., Z. Phys. **C11** (1982) 315
R.K. Ellis, D.A. Ross, E.A. Terrano, Phys. Rev. Lett. **45**(1980) 1225;
Nucl. Phys. **B178**(1981) 421
J.A.M. Vermaseren, K.J.F. Gaemers, S.J. Oldham, Nucl. Phys. **B187** (1981) 301
T.D. Gottschalk, Phys. Lett. **109B** (1982) 331
T.D. Gottschalk and M.P. Shatz, CALT-68-1172,-1173,-1199;
Phys. Lett. **150B** (1985) 451
G. Kramer and B. Lampe, Fortschr. Phys. **37** (1989) 161,
Z. Phys. **C34** (1987)497, erratum-ibid.**C42** (1989) 504.

[26] F. Gutbrod et al., see Ref. [25].

[27] R.K. Ellis et al., see Ref. [25]
The actual implementation of this matrix element into the LUND Monte Carlo was based on the work of Kunzst, Ali, Barreiro, and Zhu (see Ref. [25]). It uses the P-recombination scheme.

[28] T. Sjöstrand, Int. J. Mod. Phys., **A3** (1988) 751.

[29] G. Altarelli and G. Parisi, Nucl. Phys. **B216**(1977)298.

[30] W. de Boer, H.Fürstenau and J.H.Köhne, . IEKP – KA/90-4, submitted to Z. Phys. C.

[31] JADE Collab., S. Bethke et al., Phys. Lett. **213B** (1988) 235
TASSO Collab., W. Braunschweig et al., Phys. Lett. **214B** (1988) 286
AMY Collab., I.H. Park et al., Phys. Rev. Lett. **62** (1989) 1713
S. Bethke, Z. Phys. **C43** (1989) 331
MARK-II Collab., S. Bethke et al., Z. Phys. **C43** (1989) 325
OPAL Collab., M.Z. Akrawy et al., Phys. Lett. **235B** (1990) 389
VENUS Collab., K. Abe et al., Phys. Lett. **B240** (1990) 232
DELPHI Collab., P. Abreu et al., CERN-EP/90-89
JADE Collab., N. Magnussen et al., DESY 90-089.

[32] TASSO Collab., Z. Phys. **C41**(1988) 359.

[33] MARK-II Coll., A. Petersen et al., Phys. Rev. **D37** (1988) 1.

[34] OPAL Collab., M.Z. Akrawy, et al., CERN-EP/90-94.

[35] A. Bassetto, M. Ciafaloni, G. Marchesini, A.H. Mueller,
Nucl. Phys. **B207**(1982)189
Yu.L. Dokshitser, V.S. Fadin, V.A. Khoze,
Phys. Lett. **115B** (1982) 242; Z. Phys. **C18** (1983) 37
Yu.L. Dokshitzer, V.A. Khoze, S.I. Troyan, and A.H. Mueller, Rev. Mod. Phys. **60** (1988) 373
Yu.L. Dokshitzer, V.A. Khoze, G. Marchesini, B.R. Webber, CERN-TH-5738/90; CERN-TH-5694/90.

[36] JADE Collab., W. Bartel et al.,
Phys. Lett. **B101** (1981) 129; Z. Phys **C21** (1983) 37
TPC/2γ Collab., H. Aihara et al., Z. Phys. **C28** (1985) 31
TASSO Collab., M. Althoff et al., Z. Phys. **C29** (1985) 29
MARK-II Collab., P.D. Sheldon et al., Phys. Rev. Lett. **57** (1986) 139
AMY Collab., Y.K. Kim et al., Phys. Rev. Lett. **63** (1989) 1772.

[37] M. Derrick et al., Phys. Lett. **165B**(1985) 449
K. Sugano, Int. J. Mod. Phys. **A3**(1988) 2249
JADE Collab., W. Bartel et al., Phys. Lett. **123B** (1983) 460
TPC Collab., R.J. Madaras et al., Rencontre de Moriond on Strong Interactions and Gauge Theories, Les Arcs (1986)
CELLO Collab., contributed paper at the International Symp. on Lepton and Photon Interactions at High Energies, Hamburg, 1987
AMY Collab., Y.K. Kim et al., KEK 89-44, Phys.Rev.Lett. **63** (1989) 1772.
MARK-II Collab., A. Petersen et al., Phys. Rev. Lett. **55** (1985) 1954
TASSO Collab., W. Braunschweig et al., DESY 89-032 Z.Phys. **C45** (1989) 1.

[38] DELPHI Collab., P. Abreu, et al., contributed paper to the Int. Conf. on High Energy Phys., Singapore, 1990.

[39] T.Sjöstrand, private communication.

[40] Ya.I. Azimov et al., Phys. Lett. **B165** (1985) 147.

[41] V.A. Khoze, priv. communication.

[42] M.Bengtsson and T. Sjöstrand, Nucl. Phys. **B289** (1987) 810.

[43] Yu.L. Dokshitzer et al., CERN-TH.5738/90.

[44] G. Ballocchi, R. Odorico, CERN-EP/89-162, Submitted to Nucl.Phys.B.

[45] P. Biddulph and G. Thompson, Comput. Phys. Commun. **54**(1989) 13.

[46] S. Bethke, Z. Phys. **C43** (1989) 331.
Invited talk at the XX. Int. Symposium on Multiparticle Dynamics, Dortmund, Sept. 1990

[47] JADE Collab., W. Bartel et al., Z. Phys. **C33** (1986) 23.

[48] S. Bethke, Invited talk at the QCD'90, Montpellier, France, July, 1990

[49] OPAL Collab., M.Z. Akrawy, et al., Phys. Lett. **B235** (1990) 389.

[50] DELPHI Collaboration, P. Abreu, et al., CERN-EP-90-89, Submitted to Phys.Lett.B.

[51] L3 Collaboration, B. Adeva, et al., L3-011.

[52] MARK-II Collab., S. Komamiya et al., Phys. Rev. Lett. **64** (1990) 987.

[53] OPAL Collab., M.Z. Akrawy, et al. CERN-PPE/90-143, subm. to Z. Phys. C.

[54] W.J. Marciano, Phys. Rev. **D29** (1984) 580.

[55] M. Dine, J. Sapirstein, Phys. Rev. Lett. **43** (1979) 668
K.G. Chetyrkin et al., Phys. Lett. **B85** (1979) 277
W. Celmaster, R.J. Gonsalves, Phys. Rev. Lett. **44** (1979) 560.

[56] G. Grunberg, Phys. Rev. **D29** (1984) 2315.

[57] P.M. Stevenson, Phys. Rev. **D23** (1981) 2916.

[58] S. Brodsky, G.L. Lepage and P.B. Mackenzie, Phys. Rev. **D28** (1983) 228.

[59] Z. Kunszt, P. Nason, G. Marchesini and B.R. Webber, QCD, Proc. of the 1989 Workshop on Z Physics at LEP 1, CERN 89-08, Vol. 1, p.373, Eds. G. Altarelli, R. Kleiss and C. Verzegnassi.

[60] A. Ali, F. Barreiro, Phys. Lett. **118B** (1982) 155, Nucl. Phys. **B236** (1984) 269.

[61] G. Kramer and B. Lampe, see Ref. [25].

[62] G. Kramer and N. Magnussen, DESY 90-080, subm. Z. Phys.

[63] C.L. Basham, L.S. Brown, S.D. Ellis, S.T. Love, Phys. Rev. **D17** (1978) 2298, Phys. Rev. Lett. **41** (1978) 1585, Phys. Rev. **D19** (1979) 2018.

[64] S.D. Ellis, D.G. Richards, W.J. Stirling, Phys. Lett. **119B** (1982) 193, Nucl. Phys. **B229** (1983) 317.

[65] N.K. Falck and G. Kramer, Z. Phys. **C42** (1989) 459.

[66] PLUTO Collab., C. Berger et al., Phys. Lett. **90B** (1980) 312, Z. Phys. **C12** (1982) 297
MARK-J Collab., B. Adeva et al., Phys. Rev. Lett. **49** (1982) 521, Phys. Rev. Lett. **50** (1983) 2051
CELLO Collab., H.-J. Behrend et al., Nucl. Phys. **B218** (1983) 269, Phys. Lett. **138B** (1984) 311
JADE Collab., W. Bartel et al., Z. Phys. **C25** (1984) 231
MAC Collab., E. Fernandez et al., Phys. Rev. **D31** (1985) 2724
TASSO Collab., Braunscheig et al., Z. Phys. **C36** (1987) 349
MARK-II Collab., D.R. Wood et al., Phys. Rev. **D37** (1988) 3091
TOPAZ Collab., I. Adachi et al., Phys. Lett. **227B** (1989) 495.

[67] DELPHI Collab., P. Abreu et al., CERN-PPE/90-122.

[68] OPAL Collab., M.Z. Akrawy et al., CERN-PPE/90-121.

[69] J. Körner et al., Nucl. Phys. **B185** (1981) 365.

[70] M. Bengtsson and P.M. Zerwas, Phys. Lett. **208B** (1988) 306
M. Bengtsson, Z. Phys. **C42** (1989) 75.

[71] O. Nachtman and A. Reiter, Z. Phys. **C16** (1982) 45.

[72] S. Bethke, A. Ricker, and P.M. Zerwas, PITHA 90/14.

[73] K.-H. Müller, to be publ. in Proc. of 25th Int. Conf. on High Energy Phys., Singapore, 1990
M. Hahn, Talk at the QCD'90, Montpellier, July, 1990.

[74] VENUS Coll., K. Abe et al., KEK 90-62.

[75] AMY Coll., I.H. Park et al., Phys. Rev. Lett. **62** (1989) 1713.

[76] L3 Collaboration, B. Adeva, et al., L3-012.

[77] OPAL Coll., M.Z. Akrawy et al., CERN-PPE/90-097.

[78] DELPHI Coll., P. Abreu et al., Contributed paper to 25th Int. Conf. on High Energy Phys., Singapore, 1990.

[79] G. Rudolph, Physics at LEP, CERN 86-02 (1986), Vol. 2, 150.

[80] G. Altarelli, Ann. Rev. Nucl. Part. Sci. **39** (1989) 357.